LA-UR-13-26757
Approved for public release; distribution is unlimited.

Title: TRX Plug and Socket Proximity Detection Methodology - Preliminary

Author(s): Durkee, Joe W. Jr.
Johns, Russell C.

Intended for: Report

Issued: 2013-08-28

TRX Plug and Socket Proximity Detection Methodology
Preliminary

Joe W. Durkee, Jr. and Russell C. Johns
Los Alamos National Laboratory
jdurkee@lanl.gov
505-665-0530
Fax: 505-665-2897
PO Box 1663, MS C921
Los Alamos, NM 87545

ABSTRACT

The TRX code is being developed at Los Alamos National Laboratory to modernize the development, execution, and interpretation of radiation-transport calculations that are executed using the MCNP6 code. As part of this development, a graphics-driven interface is being created to facilitate menu-driven geometry creation using geometrical objects such as boxes, cylinders, and spheres. To aid the user and automate MCNP6 input deck preparation, algorithmic assessment of object proximity is needed. In this article, we present the algorithms that are being used in TRX for proximity detection. The algorithms are also designed to provide a prescription to reposition an object that is determined to collide with another object. With one exception, these deterministic algorithms are analytic expressions that are derived using trigonometry and analytic geometry. In the exceptional case, the method of Lagrange multipliers yields two bivariate quadratic expressions that must be solved numerically. The algorithms are designed to have millisecond performance.

KEYWORDS: MCNP6; TRX; geometry; proximity; collision; intersection.

Contents

Figures

Acronyms

BOX	MCNP6 arbitrarily oriented box macrobody
LANL	Los Alamos National Laboratory
MCNP6	LANL Monte Carlo radiation transport code
RCC	MCNP6 right circular cylinder macrobody
SPH	MCNP6 sphere macrobody
TRX	LANL graphical interface tool for MCNP6

1. INTRODUCTION

The TRX code is being created to enable model development and execution through a graphical user interface. As part of this effort, capability must be developed to permit the creation and placement of boxes (BOX), finite right cylinders (RCC), and spheres (SPH) in a region of space. Intelligence must be developed to check the proximity of these objects and determine whether these objects intersect, or collide, with each other. This determination impacts the treatment of objects by MCNP6 in terms of geometry plotting and particle transport.

Historically, the determination of object proximity has been made by the user during MCNP6 input preparation. In addition, the MCNP6 geometry plotting feature can be used to inspect geometry. This feature utilizes a clever combinatorial geometry/Boolean algebra technique to assess geometrical relationships. The geometry plotting treatment used in MCNP6 (Durkee, 2012) is not appropriate for TRX because it is designed to determine intersections of surfaces with each other and the plot plane and draw the resulting curves at a number of points sufficient to give curves that are visually pleasant. There is no information regarding object proximity other than that generated for a designated plot.

MCNP6 geometry can also be assessed using particle transport to detect flaws. This can be done in a pre-calculation mode by voiding the geometry and flooding the model with particles. Or, it will be done as particles are transported during a calculation with all materials present. The MCNP6 particle-transport treatment is not appropriate for TRX geometry assessment because it is used to determine whether a particle crosses a surface from one portion of the geometry to

another. Proximity assessment is thus done only at specific points as particles are transported. Portions of the geometry may not experience particle transport, so geometry may not be suitably assessed.

Neither of these MCNP6 geometry treatments is designed to identify object surface proximity as required by TRX. Consequently, we have developed proximity assessment algorithms for TRX. For purposes of implementation in TRX, two sets of algorithms are developed. Set 1 is used to determine whether two objects intersect when they are in their optimal configuration. Using MCNP6 terminology, this means assessing objects using their local-coordinate characterizations. This is the simplest, quickest way to assess whether an object fits inside another object.

Set 2 is used to determine whether two objects intersect when they are in their arbitrary location and orientation. Using MCNP6 terminology, this means assessing objects in their global-coordinate location and orientation. This is the more complicated treatment, and requires a number of expressions and procedures to assess surface intersections.

The algorithms to be developed must provide suitably characterized intersection assessment. We seek analytic, closed-form, deterministic algorithms that should execute with millisecond performance so as to be imperceptible to the user.

In the following section, expressions for optimal geometries are developed. Section 3 addresses the derivations for objects with arbitrary location and orientation. Algorithms are

developed for BOX, RCC, and SPH macrobodies. We refer to these formulations as proximity-detection schemes (PDSs).

2. PROXIMITY DETERMINATION FOR OPTIMAL ORIENTATION

The Set 1 formulations are used to characterize whether an object fits inside of another object when both objects are in their optimal orientations.

2.1. BOX in BOX

Consider BOX A to be defined by 6 planes parallel to the *x*–*z*, *y*–*z*, and *x*–*y* planes as illustrated in Fig. 1.

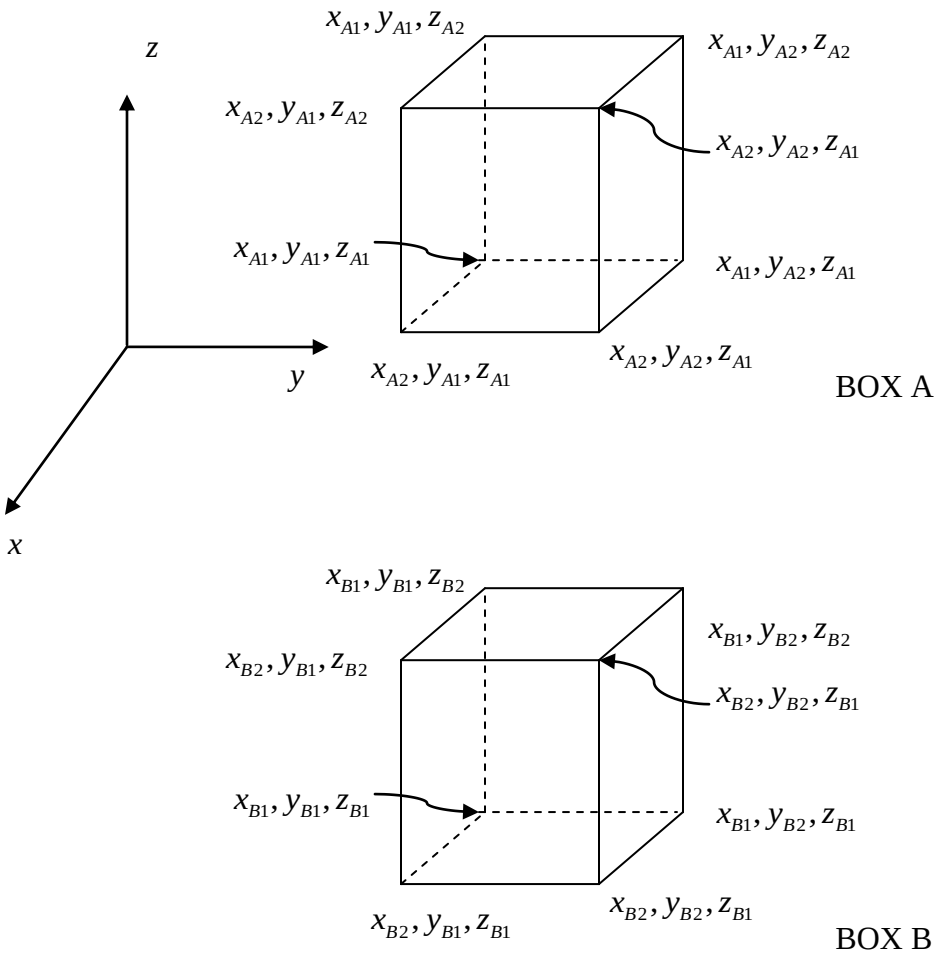

Figure 1. Two boxes.

Then

$$\begin{aligned} px_{A1} &= x_{A1}, \quad px_{A2} = x_{A2} \\ py_{A1} &= y_{A1}, \quad py_{A2} = y_{A2} \\ pz_{A1} &= z_{A1}, \quad pz_{A2} = z_{A2} \end{aligned} \tag{1}$$

Similarly, for BOX B

$$\begin{aligned} px_{B1} &= x_{B1}, \quad px_{B2} = x_{B2} \\ py_{B1} &= y_{B1}, \quad py_{B2} = y_{B2} \\ pz_{B1} &= z_{B1}, \quad pz_{B2} = z_{B2} \end{aligned} \tag{2}$$

For BOX A to fit inside of BOX B,

$$\begin{aligned} px_{A1} > px_{B1} \text{ and } px_{A2} < px_{B2}, \\ py_{A1} > py_{B1} \text{ and } py_{A2} < py_{B2}, \\ pz_{A1} > pz_{B1} \text{ and } pz_{A2} < pz_{B2}. \end{aligned} \tag{3}$$

For BOX B to fit inside of BOX A,

$$\begin{aligned} px_{A1} < px_{B1} \text{ and } px_{A2} > px_{B2}, \\ py_{A1} < py_{B1} \text{ and } py_{A2} > py_{B2}, \\ pz_{A1} < pz_{B1} \text{ and } pz_{A2} > pz_{B2}. \end{aligned} \tag{4}$$

2.2. BOX in RCC

The expressions for the BOX Are given in Eq.(1). If the RCC is taken to be centered on the *x*-axis, then

$$y^2 + z^2 + R_B^2. \tag{5}$$

In order that the BOX fit inside the RCC, it is required that

$$\begin{aligned} px_{A1} < px_{B1} \text{ and } px_{A2} > px_{B2}, \\ R_1 < R_B \text{ and } R_2 < R_B \text{ and } R_3 < R_B \text{ and } R_4 < R_B \end{aligned} \tag{6}$$

where the radii $R_1, R_2, R_3,$ and R_4 are defined as

$$\begin{aligned} R_1 &= \left(y_{A2}^2 + z_{A2}^2 \right)^{1/2}, \\ R_2 &= \left(y_{A1}^2 + z_{A2}^2 \right)^{1/2}, \\ R_3 &= \left(y_{A2}^2 + z_{A1}^2 \right)^{1/2}, \\ R_4 &= \left(y_{A2}^2 + z_{A1}^2 \right)^{1/2}. \end{aligned} \tag{7}$$

Figure 2 shows a cross section of the BOX and RCC.

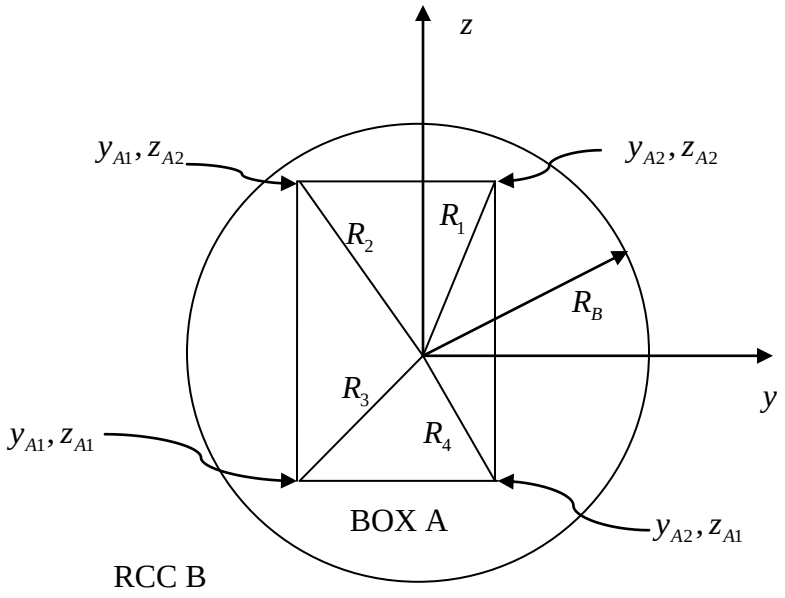

Figure 2. BOX in RCC.

2.3. RCC in BOX

The equations of RCC A centered on the *x*-axis is

$$y^2 + z^2 + R_A^2, \tag{8}$$

while the equation for BOX B is given by Eq.(2). In order that the RCC fit inside the BOX, it is required that

$$\begin{aligned} &px_{A1} > px_{B1} \text{ and } px_{A2} < px_{B2}, \\ &R_A < |y_{B1}| \text{ and } R_A < |y_{B2}| \text{ and } R_A < |z_{B1}|_B \text{ and } R_A < |z_{B2}| \end{aligned} \tag{9}$$

Figure 3 shows a cross section of the BOX and RCC.

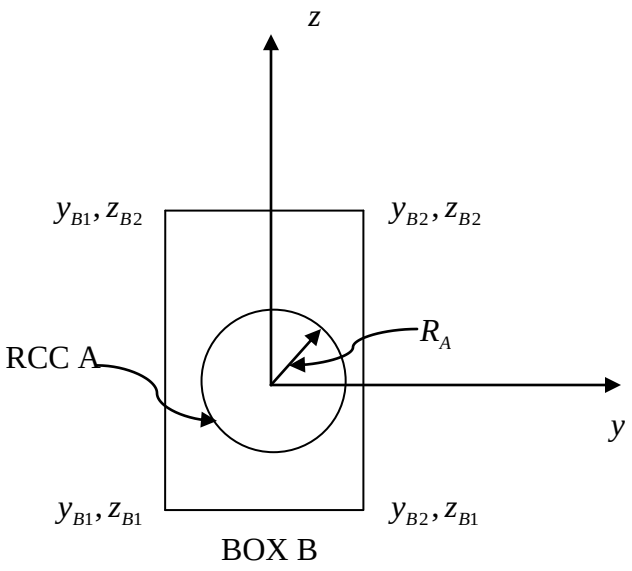

Figure 3. RCC in BOX.

2.4. BOX in SPH

This formulation is similar to the BOX in RCC discussed in Section 2.2 and illustrated in Fig. 2. The equations defining BOX A are given in Eq.(1). The equation of SPH B centered at the origin is

$$x^2 + y^2 + z^2 = R_B^2. \tag{10}$$

In order that the BOX fit inside the SPH, it is necessary that

$$R_{Axz} < R_B \text{ and } R_{Ayz} < R_B, \tag{11}$$

where

$$\begin{aligned} R_{Axz} &= \left(x_{A1}^2 + z_{A1}^2 \right)^{1/2} \\ R_{Ayz} &= \left(y_{A1}^2 + z_{A1}^2 \right)^{1/2}. \end{aligned} \tag{12}$$

2.5. SPH in BOX

The formulations resemble those for an RCC in a BOX discussed in Section 2.3 and illustrated in Fig. 3. The equations defining BOX B are given in Eq.(2). The equation of SPH A centered at the origin is

$$x^2 + y^2 + z^2 = R_A^2. \tag{13}$$

In order that the SPH fit inside the BOX, the conditions

$$R_A < |y_{B1}| \text{ and } R_A < |y_{B2}| \text{ and } R_A < |z_{B1}|_B \text{ and } R_A < |z_{B2}| \tag{14}$$

must be satisfied.

2.6. RCC in RCC

The equations of RCCs A and B are given in Eqs.(8) and (5), respectively. The conditions needed so that RCC A fits in RCC B are

$$px_{A1} > px_{B1} \text{ and } px_{A2} < px_{B2} \text{ and } R_A < R_B. \tag{15}$$

2.7. RCC in SPH

The equations of RCC A and sphere B are given in Eqs.(8) and (10), respectively. The conditions required for RCC A to fit in SPH B are

$$R_A < R_B \text{ and } R_1 < R_A \text{ and } R_2 < R_A \tag{16}$$

2.8. SPH in RCC

The equations of SPH A and RCC B are given in Eqs.(13) and (5), respectively. The conditions so that SPH A fits in RCC B are

$$R_A > R_B \text{ and } R_A < |x_{B1}| \text{ and } R_A < |x_{B2}| . \quad (17)$$

2.9. SPH in SPH

This PDS is the simplest for the objects under consideration. The equations of SPH A and SPH B are given in Eqs.(13) and (10), respectively. The condition so that SPH A fits in RCC B is

$$R_A < R_B . \quad (18)$$

3. PROXIMITY DETERMINATION FOR OBJECTS WITH ARBITRARY LOCATION AND ORIENTATION

The formulations for Set 2 are developed to ascertain the proximity of two objects having arbitrary location and orientation. These formulations determine the intersection, if any, of a three-dimensional (3-D) surface with another 3-D surface. These PDSs are much lengthier and more complicated than those for Set 1. Nevertheless, the PDSs are straightforward applications of trigonometry and analytic geometry. In one instance, the PDS uses the method of Lagrange multipliers. To better convey the concepts, each PDS is presented using itemized descriptions followed by development of the requisite equations.

3.1. BOX and BOX

Proximity determination for two boxes is made using the planes and lines along each edge of the boxes. In essence, the intersection of each of the 12 lines along the edges of BOX B with each of the 6 planes defining BOX A is determined. The planes defining the surfaces of BOX A

are infinite in extent. Checks are then made to determine whether each point of intersection lies within the extent of BOX A. Figure 4 illustrates a box colliding with another box.

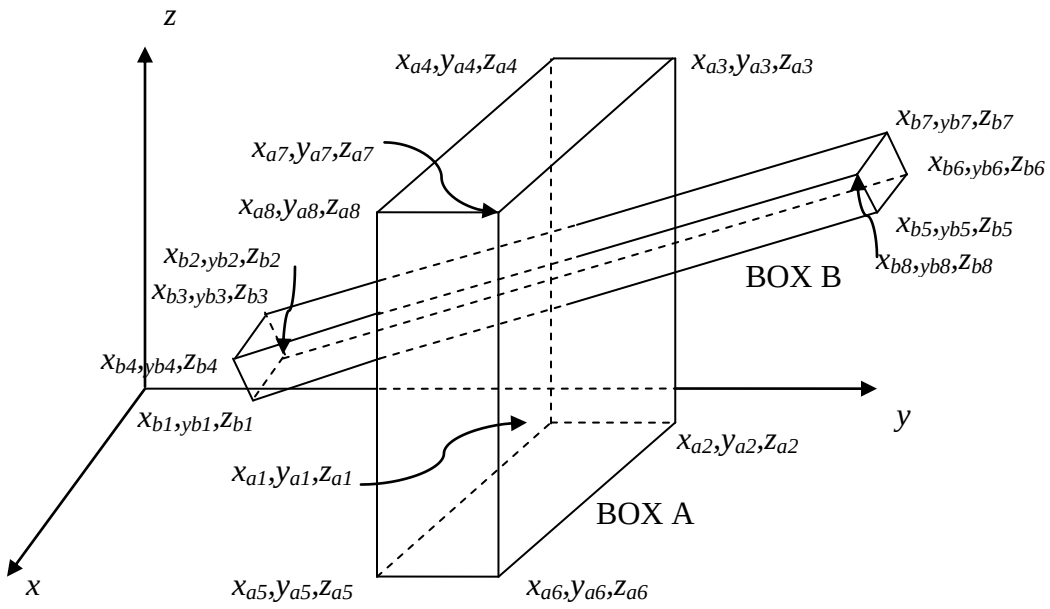

Figure 4. Collision of two boxes.

Each BOX has 6 sides and 12 lines along its edges. These characteristics are used to devise the PDS for two boxes is:

1. Determine the equation of the plane for each side of BOX A.
2. Determine the equation of the line along each edge of BOX B.
3. Attempt to determine the POI of each plane of BOX A with each line of BOX B.
4. For each POI, determine whether the POI for the plane lies within the BOX A portion of the plane.

The equation of the planes π_{Ai} on each of the six sides *i* of BOX A can be specified in terms of the dot product of the normal vector $\vec{A}_i^N$ to the plane and a vector in the plane as shown in Fig. 5 (Tierney, 1974). The vector in the plane can be defined using the point $\vec{P}(x, y, z)$ in the plane and the point $\vec{P}_{Ai}(x_{Ai}, y_{Ai}, z_{Ai})$ at a vertex point in plane *i*.

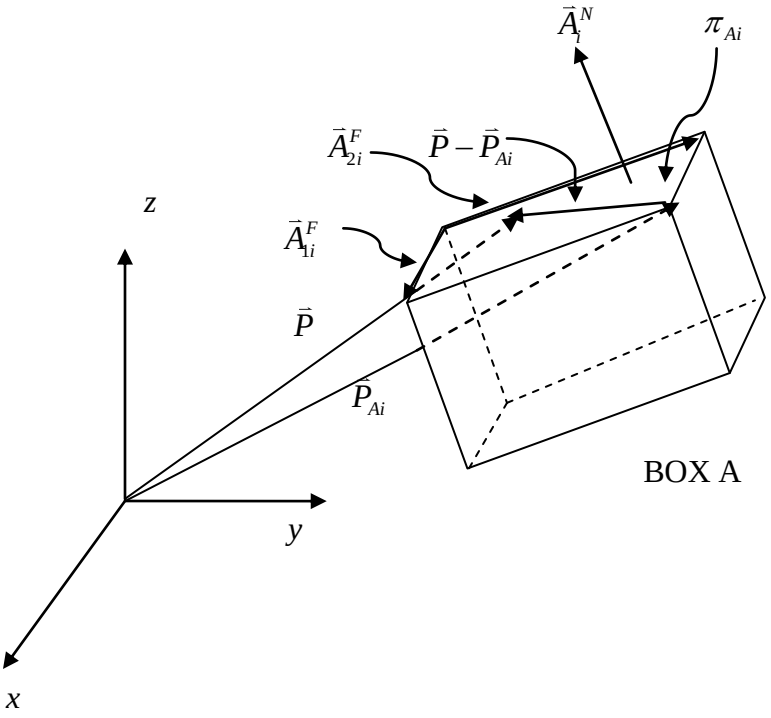

Figure 5. Vector specification of plane π_{Ai} for BOX A.

So

$$\pi_{Ai} : \vec{A}_i^N \cdot \left(\vec{P} - \vec{P}_{Ai} \right) = 0, \quad i = 1, \ldots 6 , \tag{19}$$

where

$$\vec{P} = x\hat{i} + y\hat{j} + z\hat{k} , \tag{20}$$

and

$$\vec{P}_{Ai} = x_{Ai}\hat{i} + y_{Ai}\hat{j} + z_{Ai}\hat{k} . \tag{21}$$

Expanding Eqs.(19)–(21) and rearranging,

$$a_{Ai}^{N}x+b_{Ai}^{N}y+c_{Ai}^{N}z=d_{Ai}^{N}, \tag{22}$$

where

$$d_{Ai}^{N}=a_{Ai}^{N}x_{Ai}+b_{Ai}^{N}y_{Ai}+c_{Ai}^{N}z_{Ai}. \tag{23}$$

The normal $\vec{A}_i^N$ is determined using the cross product of two vectors $\vec{A}_{1i}^F$ and $\vec{A}_{2i}^F$ on face *i* of BOX A, where

$$\vec{A}_{1i}^F=a_{1i}^F\hat{i}+b_{1i}^F\hat{j}+c_{1i}^F\hat{k}, \tag{24}$$

and

$$\vec{A}_{2i}^F=a_{2i}^F\hat{i}+b_{2i}^F\hat{j}+c_{2i}^F\hat{k}. \tag{25}$$

The coefficients of these vectors are selected using points located at three vertices on each planar side of BOX A. Using the designations in Fig. 1, the coefficients for $\vec{A}_{1i}^F$ are defined as

$$\begin{array}{lll}
a_{21}^F=x_{A4}-x_{A1}, & b_{11}^F=y_{A4}-y_{A1}, & c_{11}^F=z_{A4}-z_{A1}\\
a_{22}^F=x_{A8}-x_{A5}, & b_{12}^F=y_{A8}-y_{A5}, & c_{12}^F=z_{A8}-z_{A5}\\
a_{23}^F=x_{A4}-x_{A1}, & b_{13}^F=y_{A4}-y_{A1}, & c_{13}^F=z_{A4}-z_{A1}\\
a_{24}^F=x_{A3}-x_{A2}, & b_{14}^F=y_{A3}-y_{A2}, & c_{14}^F=z_{A3}-z_{A2}\\
a_{25}^F=x_{A5}-x_{A1}, & b_{15}^F=y_{A5}-y_{A1}, & c_{15}^F=z_{A5}-z_{A1}\\
a_{26}^F=x_{A8}-x_{A4}, & b_{16}^F=y_{A8}-y_{A4}, & c_{16}^F=z_{A8}-z_{A4}
\end{array}, \tag{26}$$

and for $\vec{A}_{2i}^F$ are

$$\begin{array}{lll}
a_{11}^F=x_{A2}-x_{A1}, & b_{11}^F=y_{A2}-y_{A1}, & c_{11}^F=z_{A2}-z_{A1}\\
a_{12}^F=x_{A6}-x_{A5}, & b_{12}^F=y_{A6}-y_{A5}, & c_{12}^F=z_{A6}-z_{A5}\\
a_{13}^F=x_{A5}-x_{A1}, & b_{13}^F=y_{A5}-y_{A1}, & c_{13}^F=z_{A5}-z_{A1}\\
a_{14}^F=x_{A6}-x_{A2}, & b_{14}^F=y_{A6}-y_{A2}, & c_{14}^F=z_{A6}-z_{A2}\\
a_{15}^F=x_{A2}-x_{A1}, & b_{15}^F=y_{A2}-y_{A1}, & c_{15}^F=z_{A2}-z_{A1}\\
a_{16}^F=x_{A3}-x_{A4}, & b_{16}^F=y_{A3}-y_{A4}, & c_{16}^F=z_{A3}-z_{A4}
\end{array}. \tag{27}$$

The normal vector to plane π_{Ai} is given by

$$\vec{A}_i^N=\vec{A}_{1i}^F\times\vec{A}_{2i}^F=a_{Ai}^N\hat{i}+b_{Ai}^N\hat{j}+c_{Ai}^N\hat{k}, \tag{28}$$

where

$$\begin{aligned} a_{Ai}^{N} &= b_{1i}^{F} c_{2i}^{F} - c_{1i}^{F} b_{2i}^{F} \\ b_{Ai}^{N} &= c_{1i}^{F} a_{1i}^{F} - a_{1i}^{F} c_{2i}^{F} \\ c_{Ai}^{N} &= a_{1i}^{F} b_{2i}^{F} - b_{2i}^{F} a_{2i}^{F} \end{aligned} . \tag{29}$$

For Step 2, the equation of the line along each edge of BOX B is determined by considering the equation of the line $L_{Bj}^{E}(t)$ along each of the 12 edges of BOX B as given by

$$\begin{aligned} L_{Bj}^{E}(t): x &= x_{Bj} + a_{Bj}^{E} t \\ y &= y_{Bj} + b_{Bj}^{E} t, \quad j = 1,\ldots,12 \\ z &= z_{Bj} + c_{Bj}^{E} t \end{aligned} . \tag{30}$$

The point (x_{Bj}, y_{Bj}, z_{Bj}) is a vertex through which $L_{Bj}^{E}(t)$ passes. The quantities a_{Bj}^{E}, b_{Bj}^{E}, and c_{Bj}^{E} are the coefficients of the vector $\vec{B}_{j}^{E}$ along the edges of BOX B as given by

$$\vec{B}_{j}^{E} = a_{Bj}^{E} \hat{i} + b_{Bj}^{E} \hat{j} + c_{Bj}^{E} \hat{k} , \tag{31}$$

and

$$\begin{aligned} a_{B1}^{E} &= x_{B2} - x_{B1}, \quad b_{B1}^{E} = y_{B2} - y_{B1}, \quad c_{B1}^{E} = z_{B2} - z_{B1} \\ a_{B2}^{E} &= x_{B3} - x_{B2}, \quad b_{B2}^{E} = y_{B3} - y_{B2}, \quad c_{B2}^{E} = z_{B3} - z_{B2} \\ a_{B3}^{E} &= x_{B4} - x_{B3}, \quad b_{B3}^{E} = y_{B4} - y_{B3}, \quad c_{B3}^{E} = z_{B4} - z_{B3} \\ a_{B4}^{E} &= x_{B1} - x_{B4}, \quad b_{B4}^{E} = y_{B1} - y_{B4}, \quad c_{B4}^{E} = z_{B1} - z_{B4} \\ a_{B5}^{E} &= x_{B6} - x_{B5}, \quad b_{B5}^{E} = y_{B6} - y_{B5}, \quad c_{B5}^{E} = z_{B6} - z_{B5} \\ a_{B6}^{E} &= x_{B7} - x_{B6}, \quad b_{B6}^{E} = y_{B7} - y_{B6}, \quad c_{B6}^{E} = z_{B7} - z_{B6} \\ a_{B7}^{E} &= x_{B8} - x_{B7}, \quad b_{B7}^{E} = y_{B8} - y_{B7}, \quad c_{B7}^{E} = z_{B8} - z_{B7} \\ a_{B8}^{E} &= x_{B5} - x_{B8}, \quad b_{B8}^{E} = y_{B5} - y_{B8}, \quad c_{B8}^{E} = z_{B5} - z_{B8} \\ a_{B9}^{E} &= x_{B5} - x_{B1}, \quad b_{B9}^{E} = y_{B5} - y_{B1}, \quad c_{B9}^{E} = z_{B5} - z_{B1} \\ a_{B10}^{E} &= x_{B6} - x_{B2}, \quad b_{B10}^{E} = y_{B6} - y_{B2}, \quad c_{B10}^{E} = z_{B6} - z_{B2} \\ a_{B11}^{E} &= x_{B7} - x_{B3}, \quad b_{B11}^{E} = y_{B7} - y_{B3}, \quad c_{B11}^{E} = z_{B7} - z_{B3} \\ a_{B12}^{E} &= x_{B8} - x_{B4}, \quad b_{B12}^{E} = y_{B8} - y_{B4}, \quad c_{B12}^{E} = z_{B8} - z_{B4} \end{aligned} \tag{32}$$

Step 3 is addressed by attempting to determine the POI of the surface of BOX A with each line of BOX B. The POI for each line $L_{Bj}^{E}(t)$ with each plane of BOX A is determined. Each line will intersect the planes of BOX A unless the line and plane are parallel. The intersections are determined by inserting Eq.(30) into Eq.(22) and solving for the value of the parameter t for the intersection of each plane π_{Ai} and each line $L_{Bj}^{E}(t)$ so that

$$t_{ij} = \frac{d_{Ai}^{N} - \left(a_{Ai}^{N} x_{Bj} + b_{Ai}^{N} y_{Bj} + c_{Ai}^{N} z_{Bj} \right)}{a_{Ai}^{N} a_{Bj} + b_{Ai}^{N} b_{Bj} + c_{Ai}^{N} c_{Bj}}. \tag{33}$$

The POIs are

$$POI_{Aij} = \left[x(t_{ij}), y(t_{ij}), z(t_{ij}) \right]. \tag{34}$$

Finally, for Step 4 each POI a determination is made as to whether the POI for the plane lies within the BOX A portion of the plane. The concept is illustrated in Fig. 6.

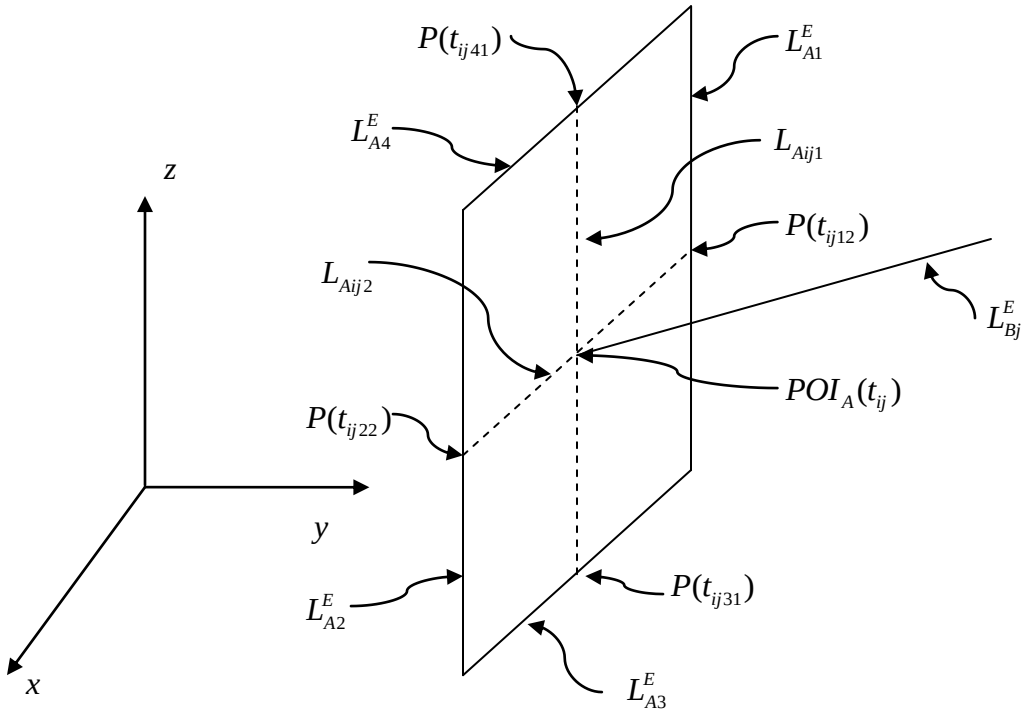

Figure 6. Intersection of a line from BOX B with a plane of BOX A.

The intersection check is done by first constructing two lines are constructed that contain $POI_{Aij} \equiv POI_A(t_{ij})$ and are oriented so that they are perpendicular to the ends of the box through which they pass. The equation of the line $L^E_{Ak}(t)$ along each of the 12 edges of BOX A is

$$\begin{aligned} L^E_{Ak}(t): x &= x_{Ak} + a^E_{Ak} t \\ y &= y_{Ak} + b^E_{Ak} t, \quad k = 1,\ldots,12\,. \\ z &= z_{Ak} + c^E_{Ak} t \end{aligned} \tag{35}$$

The point (x_{Ak}, y_{Ak}, z_{Ak}) is a vertex through which $L^E_{Ak}(t)$ passes. The quantities a^E_{Ak}, b^E_{Ak}, and c^E_{Ak} are the coefficients of the vector $\vec{A}^E_k$ along the edges of BOX A as given by

$$\vec{A}^E_k = a^E_{Ak}\hat{i} + b^E_{Ak}\hat{j} + c^E_{Ak}\hat{k}\,, \tag{36}$$

and

$$\begin{aligned}
a^E_{A1} &= x_{A2} - x_{A1}, \quad b^E_{A1} = y_{A2} - y_{A1}, \quad c^E_{A1} = z_{A2} - z_{A1} \\
a^E_{A2} &= x_{A3} - x_{A2}, \quad b^E_{A2} = y_{A3} - y_{A2}, \quad c^E_{A2} = z_{A3} - z_{A2} \\
a^E_{A3} &= x_{A4} - x_{A3}, \quad b^E_{A3} = y_{A4} - y_{A3}, \quad c^E_{A3} = z_{A4} - z_{A3} \\
a^E_{A4} &= x_{A1} - x_{A4}, \quad b^E_{A4} = y_{A1} - y_{A4}, \quad c^E_{A4} = z_{A1} - z_{A4} \\
a^E_{A5} &= x_{A6} - x_{A5}, \quad b^E_{A5} = y_{A6} - y_{A5}, \quad c^E_{A5} = z_{A6} - z_{A5} \\
a^E_{A6} &= x_{A7} - x_{A6}, \quad b^E_{A6} = y_{A7} - y_{A6}, \quad c^E_{A6} = z_{A7} - z_{A6} \\
a^E_{A7} &= x_{A8} - x_{A7}, \quad b^E_{A7} = y_{A8} - y_{A7}, \quad c^E_{A7} = z_{A8} - z_{A7} \\
a^E_{A8} &= x_{A5} - x_{A8}, \quad b^E_{A8} = y_{A5} - y_{A8}, \quad c^E_{A8} = z_{A5} - z_{A8} \\
a^E_{A9} &= x_{A5} - x_{A1}, \quad b^E_{A9} = y_{A5} - y_{A1}, \quad c^E_{A9} = z_{A5} - z_{A1} \\
a^E_{A10} &= x_{A6} - x_{A2}, \quad b^E_{A10} = y_{A6} - y_{A2}, \quad c^E_{A10} = z_{A6} - z_{A2} \\
a^E_{A11} &= x_{A7} - x_{A3}, \quad b^E_{A11} = y_{A7} - y_{A3}, \quad c^E_{A11} = z_{A7} - z_{A3} \\
a^E_{A12} &= x_{A8} - x_{A4}, \quad b^E_{A12} = y_{A8} - y_{A4}, \quad c^E_{A12} = z_{A8} - z_{A4}
\end{aligned} \tag{37}$$

The lines $L_{Aij\tilde{k}}(t)$ through POI_{Aij} are

$$
\begin{aligned}
L^E_{Aij\tilde{k}}(t): x &= x(t_{ij}) + a^E_{A\tilde{k}} u \\
y &= y(t_{ij}) + b^E_{A\tilde{k}} u, \quad i = 1,\ldots,6;\ j = 1,\ldots,12;\ \tilde{k} = 1,\ldots,12;\ \tilde{k} \neq k\,. \\
z &= z(t_{ij}) + c^E_{A\tilde{k}} u
\end{aligned}
\tag{38}
$$

The intersection of the lines $L^E_{Ak}(t)$ and $L_{Aij\tilde{k}}(t)$ are next determined. Equations (35) and (38) contain 6 equations and 5 unknowns *x*, *y*, *z*, *t*, and *u*. Therefore, a unique solution can be obtained using any 4 of the equations. Selecting the equations in *x* and *y* and solving gives

$$
t_{ijk\tilde{k}} = \frac{b^E_{A\tilde{k}}\left[x(t_{ij}) - y_{Ak}\right] - a^E_{A\tilde{k}} y(t_{ij})}{a^E_{Ak} + a^E_{A\tilde{k}} b^E_{Ak}},
\tag{39}
$$

and

$$
u_{ijk\tilde{k}} = \frac{y_{Ak} - b^E_{Ak} t_{ijk\tilde{k}} - y(t_{ij})}{b^E_{A\tilde{k}}},
\tag{40}
$$

for BOX A sides $i = 1,\ldots,6$, BOX B lines $j = 1,\ldots,12$, BOX A lines through POI_{Aij} $k = 1,\ldots,12$, and lines $\tilde{k} = 1,\ldots,12$ along the sides of BOX A. The intersection conditions for these lines are

$$
\begin{aligned}
t_{ijk\tilde{k}} < t_{ij} < t_{ijk+1\tilde{k}}, &\text{"forwards"} \\
t_{ijk\tilde{k}} > t_{ij} > t_{ijk+1\tilde{k}}, &\text{"backwards"}\,.
\end{aligned}
\tag{41}
$$

3.2. BOX and RCC

The BOX-RCC PDS analysis consists of two checks. The PDS for BOX B colliding with RCC A is:

1. First, intersections between the BOX and cylindrical portion of the RCC are determined.
2. Second, intersections between the BOX and the planes at the ends of the RCC are determined.

Figure 7 illustrates a box colliding with a cylinder.

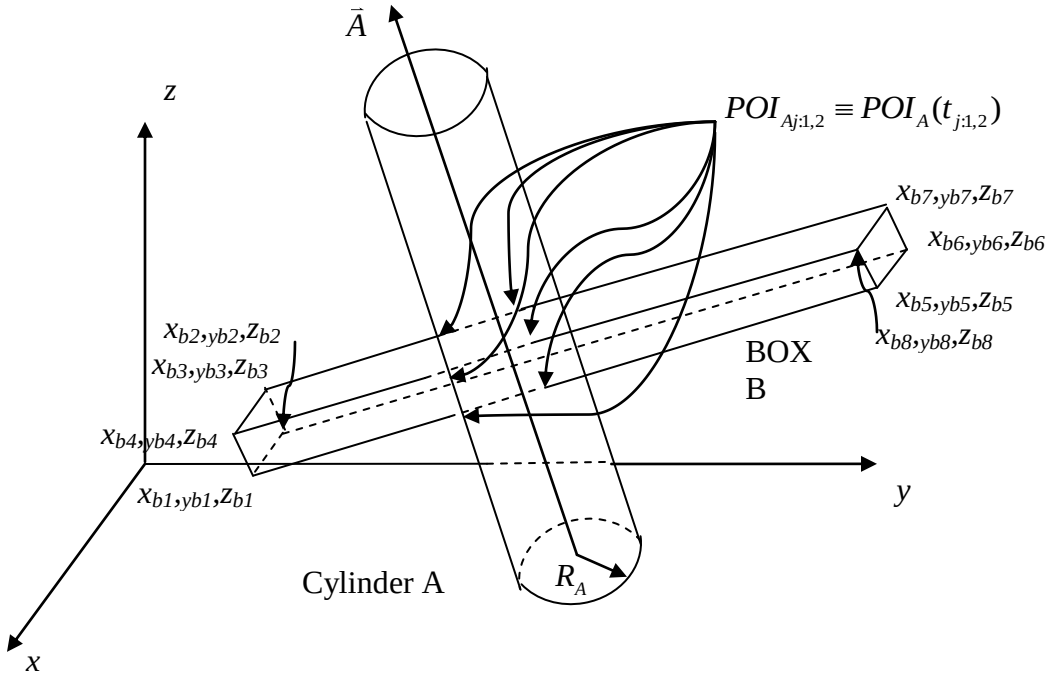

Figure 7. Collision of a box with a cylinder.

Determination of the intersection of BOX B with the cylindrical surface of RCC A is made by first considering the equation of the cylinder. The equation of a general cylinder can be written as (Brown, 2003).

$$Ax^2 + By^2 + Cz^2 + Dxy + Eyz + Fzx + Gx + Hy + Jz + K = 0\,. \qquad (42)$$

We write Eq.(42) for cylinder A as

$$A_A x^2 + B_A y^2 + C_A z^2 + D_A xy + E_A yz + F_A zx + G_A x + H\ y + J\ z + K_A = 0\,, \qquad (43)$$

To determine the POIs, the equation of a line along each edge of BOX B in Eq.(30) is inserted into Eq.(43). The resulting quadratic expression in *t* is then solved to give the two values $t_{j:1,2}$ for the POIs for each line *j* and the cylinder as

$$t_{j:1,2} = \frac{-\tilde{b}_j \pm \sqrt{\tilde{b}_j^2 - 4\tilde{a}_j\tilde{c}_j}}{2\tilde{a}_j}, \tag{44}$$

where

$$\begin{aligned}
\tilde{a}_j &= A_A\left(a_{Bj}^E\right)^2 + B_A\left(b_{Bj}^E\right)^2 + C_A\left(c_{Bj}^E\right)^2 + D_A a_{Bj}^E b_{Bj}^E + E_A b_{Bj}^E c_{Bj}^E + F_A c_{Bj}^E a_{Bj}^E \\
\tilde{b}_j &= 2A_A x_{Bj} a_{Bj}^E + 2B_A y_{Bj} b_{Bj}^E + 2C_A z_{Bj} c_{Bj}^E + D_A\left(x_{Bj} b_{Bj}^E + y_{Bj} a_{Bj}^E\right) + E_A\left(y_{Bj} c_{Bj}^E + z_{Bj} b_{Bj}^E\right) \\
&\quad + F_A\left(z_{Bj} a_{Bj}^E + x_{Bj} c_{Bj}^E\right) + G_A a_{Bj}^E + H_A b_{Bj}^E + J_A c_{Bj}^E \\
\tilde{c}_j &= A_A x_{Bj}^2 + B_A y_{Bj}^2 + C_A z_{Bj}^2 + D_A x_{Bj} y_{Bj} + E_A y_{Bj} z_{Bj} + F_A z_{Bj} x_{Bj} + G_A x_{Bj} + H_A y_{Bj} + J_A z_{Bj} + K_A
\end{aligned} \tag{45}$$

If $t_{j:1,2}$ is real, then line *j* the intersects with the sphere at the locations

$$POI_{Aj:1,2} \equiv POI_A(t_{j:1,2}) = x(t_{j:1,2}), y(t_{j:1,2}), z(t_{j:1,2}). \tag{46}$$

If $t_{j:1,2}$ is not real, then no intersection between line *j* and the cylinder occurs.

If no intersection between RCC A and BOX B is determined, the an assessment is made to determine whether BOX B intersects either of the planes at the ends of RCC A inside of the circle defined by the intersection of the cylinder and plane. The determination of the $POI_{Aij} \equiv POI_A(t_{ij})$ is done using the procedure presented above in Eqs.(19)–(34). Here, there are 2 planes, $i = 1, 2,$ to consider for RCC A and 16 lines, $j = 1, \ldots 16,$ to consider for BOX B.

A check whether POI_{Aij} lies inside the cylinder must be made. This is done by calculating the distance d_{ij} between each POI_{Aij} and the center of the circle x_{Ai}, y_{Ai}, z_{Ai} in planes π_{Ai} as illustrated in Fig. 8.

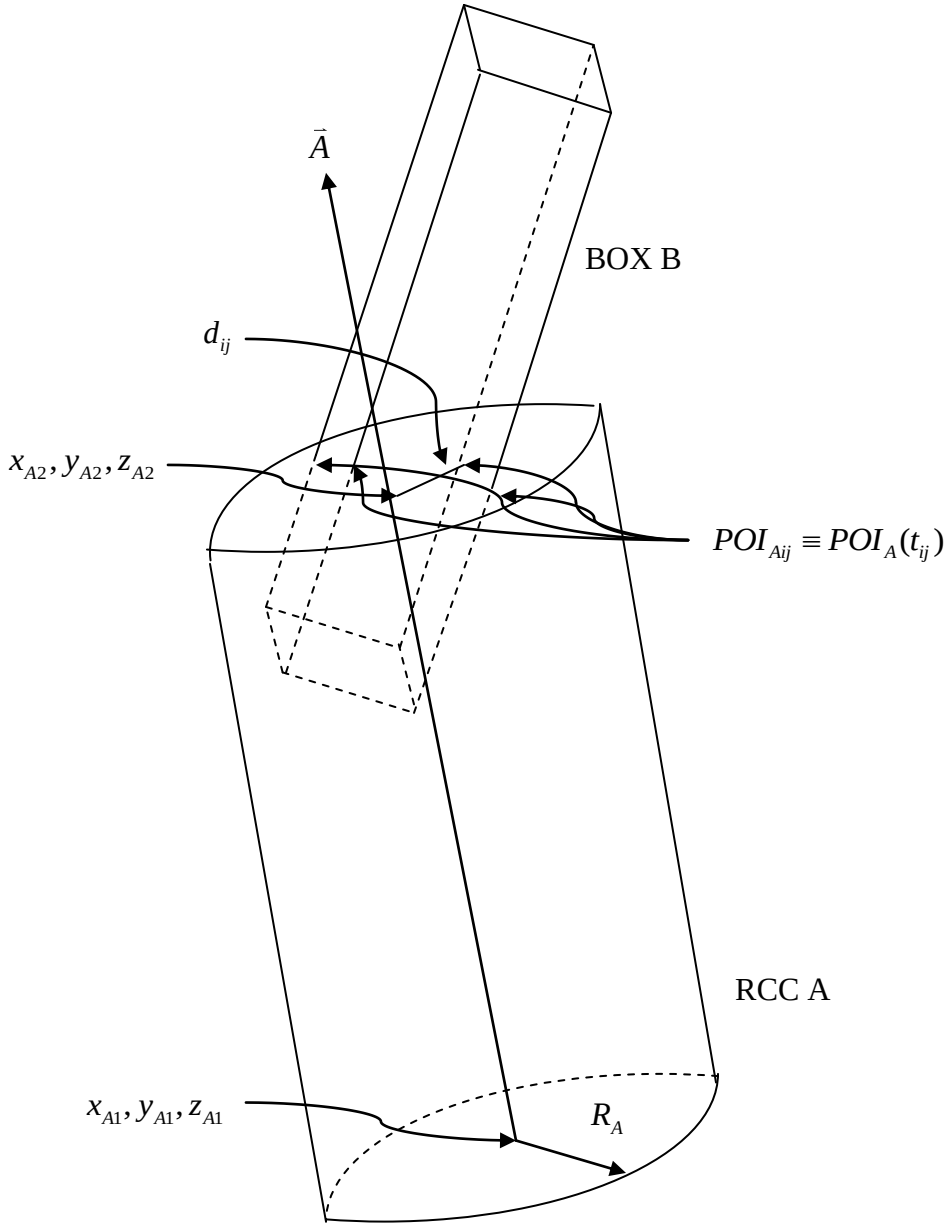

Figure 8. BOX B intersecting plane π_{A2} at the upper end of RCC A.

The distance measure is

$$d_{ij} = \left\{ \left[x(t_{ij}) - x_{Ai} \right]^2 + \left[y(t_{ij}) - y_{Ai} \right]^2 + \left[z(t_{ij}) - z_{Ai} \right]^2 \right\}^{1/2}. \tag{47}$$

The intersection assessment is

$$\begin{aligned} &d_{ij} < R_A : \text{for either i and any j then box intersects plane inside cylinder} \\ &d_{ij} > R_A : \text{for both i and all j then box does not intersect plane inside cylinder} \end{aligned} \tag{48}$$

3.3. BOX and SPH

The PDS for a box with a sphere is treated using a single determination:

1. Calculate the intersection of the lines on the edges of BOX B with sphere A.

Figure 9 illustrates a box colliding with a sphere.

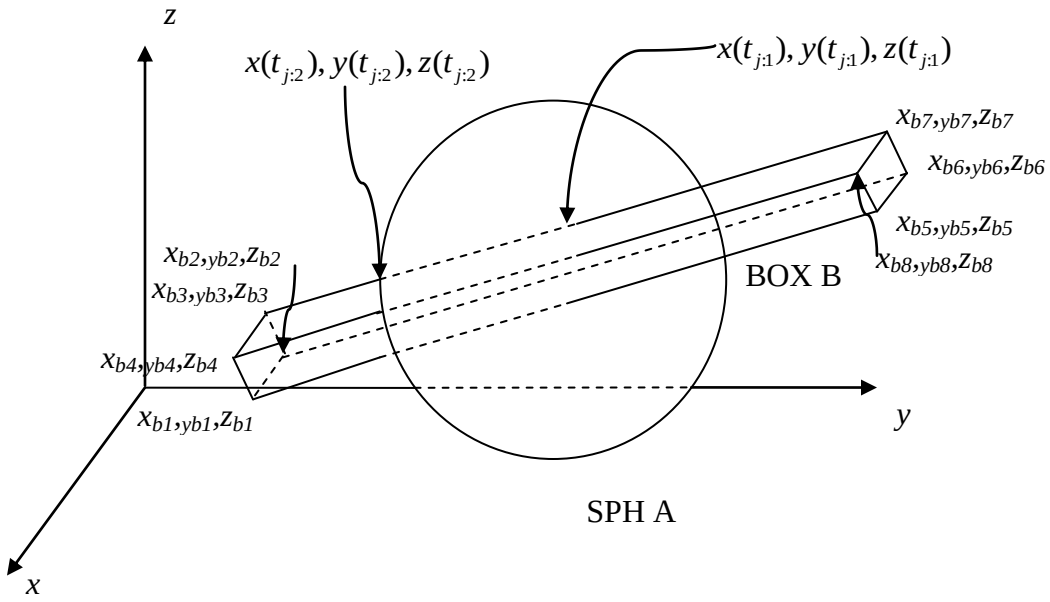

Figure 9. Collision of a box with a sphere.

The PDS formulation uses the equation of SPH A of radius R_A centered at (x_A, y_A, z_A) as given by

$$(x-x_A)^2+(y-y_A)^2+(z-z_A)^2=R_A^2. \tag{49}$$

The intersection procedure uses Eq.(30) for the equations of the lines along the edges of BOX B. Solving Eqs.(30) and (49) simultaneously gives the two values of the parameter *t* at the POIs for line *j* and the sphere as

$$t_{j:1,2}=\frac{-\tilde{b}_j\pm\sqrt{\tilde{b}_j^2-4\tilde{a}_j\tilde{c}_j}}{2\tilde{a}_j}, \tag{50}$$

where

$$\begin{aligned}\tilde{a}_j&=a_j^2+b_j^2+c_j^2\\ \tilde{b}_j&=2\left(a_jx_{1j}+b_jy_{1j}+c_jz_{1j}\right),\\ \tilde{c}_j&=x_{1j}^2+y_{1j}^2+z_{1j}^2-R_A^2\end{aligned} \tag{51}$$

and

$$\begin{aligned}x_{1j}&=x_{Bj}-x_A\\ y_{1j}&=y_{Bj}-y_A.\\ z_{1j}&=z_{Bj}-z_A\end{aligned} \tag{52}$$

If $t_{j:1,2}$ is real, then line *j* intersects the sphere. Otherwise, line *j* does not intersect the sphere.

3.4. RCC and RCC

We now consider the collision of two RCCs. The RCCs are cylinders of finite length, consisting of a cylinder and planes at either end whose orientation is perpendicular to the cylinder. The formulations must account for the finite extent of the cylinders. Figure 10

illustrates an RCC colliding with another RCC. At times in the following discussion we refer to RCCs as cylinders with the understanding that cylinders of finite length are being treated.

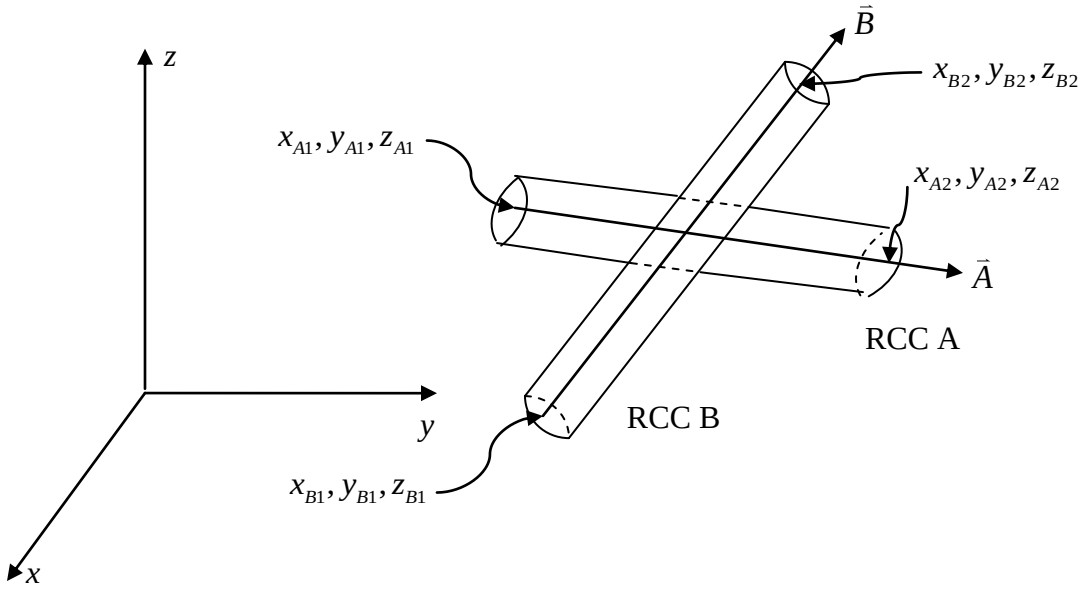

Figure 10. Collision of two RCCs.

The BOX-BOX PDS is not applicable to the collision involving two cylinders because the cylinders do not have a finite number of edges. An RCC-RCC PDS is:

1. Determine vectors $\vec{A}$ and $\vec{B}$ parallel to the axes of cylinders A and B. This implies moving the tip of $\vec{B}$ to the tip of $\vec{A}$.
2. Calculate the cross product of $\vec{A}$ and $\vec{B}$ to obtain an orthogonal vector $\vec{C}$.
3. Calculate the equation of the plane through the center of cylinder A with an orientation so that $\vec{C}$ lies in the plane.

4. Calculate the equation of the plane through the center of cylinder B with an orientation so that $\vec{C}$ lies in the plane.
5. Calculate the parametric equations of the line L_I that is parallel to $\vec{C}$ and is through the intersection of the two planes.
6. Simultaneously solve the equations for cylinder A and line L_I for the two points-of-intersection POI_{A1} and $POI_{A2.}$
7. Check whether either the points of intersection POI_{A1} or POI_{A2} for cylinder A is in cylinder B.
8. Because the cylindrical surfaces are infinite in extent, when two cylinders are found to intersect a determination must be made as to whether the intersection occurs between the ends of the RCCs.
9. If the RCCs are not found to intersect along their cylindrical surfaces, then consideration must be give to the situation where the ends of the RCCs may intersect.

The analysis will consider (1) the intersection of the cylindrical surfaces and (2) the intersection of one RCC with the plane at the end of the other RCC.

We begin with Eq.(43) for cylinder A,

$$A_A x^2 + B_A y^2 + C_A z^2 + D_A xy + E_A yz + F_A zx + G_A x + H\ y + J\ z + K_A = 0\,, \qquad (53)$$

and write a similar expression for cylinder B as

$$A_B x^2 + B_B y^2 + C_B z^2 + D_B xy + E_B yz + F_B zx + G_B x + H_B y + J_B z + K_B = 0\,, \qquad (54)$$

where coefficient subscripts A and B refer cylinders A and B, respectively. Vectors $\vec{A}$ and $\vec{B}$ parallel to the axes of cylinders A and B are first determined, where

$$\vec{A} = a_A \hat{i} + b_A \hat{j} + c_A \hat{k}, \tag{55}$$

and

$$\hat{B} = a_B \hat{i} + b_B \hat{j} + c_B \hat{k}. \tag{56}$$

The Cartesian coordinate vector coefficients are written using the points at the center of each end of the RCC so that

$$\begin{aligned} a_A &= x_{A2} - x_{A1} \\ b_A &= y_{A2} - y_{A1}, \\ c_A &= z_{A2} - z_{A1} \end{aligned} \tag{57}$$

and

$$\begin{aligned} a_B &= x_{B2} - x_{B1} \\ b_B &= y_{B2} - y_{B1}. \\ c_B &= z_{B2} - z_{B1} \end{aligned} \tag{58}$$

Next, the cross product $\vec{C}$ of $\vec{A}$ and $\vec{B}$ is calculated as

$$\vec{C} = \vec{A} \times \vec{B} = a_C \hat{i} + b_C \hat{j} + c_C \hat{k}, \tag{59}$$

where

$$\begin{aligned} a_C &= b_A c_B - c_A b_B \\ b_C &= c_A a_B - a_A c_B. \\ c_C &= a_A b_B - b_A a_B \end{aligned} \tag{60}$$

The vector $\vec{C}$ is perpendicular to $\vec{A}$ and $\vec{B}$ and, therefore, a plane containing cylinders A and B if the centerlines of these cylinders intersected. That the centerlines do not typically intersect is not important. The direction of $\vec{C}$ is important, as we see next.

For Step 3, the equation of the plane through the center of cylinder A with an orientation so that $\vec{C}$ lies in the plane is determined. The normal to this plane $\vec{N}_A$ is given by

$$\vec{N}_A = \vec{A} \times \vec{C} = a_{NA}\hat{i} + b_{NA}\hat{j} + c_{NA}\hat{k}, \tag{61}$$

where

$$\begin{aligned} a_{NA} &= b_A c_C - c_A b_C \\ b_{NA} &= c_A a_C - a_A c_C \\ c_{NA} &= a_A b_C - b_A a_C \end{aligned}. \tag{62}$$

The equation of the plane is given by the dot product of $\vec{N}_A$ and a vector in the plane from the point $P_A\left(x_{A1}, y_{A1}, z_{A1}\right)$ at the base of $\vec{A}$ and another point $P\left(x, y, z\right)$ in the plane so that

$$\vec{N}_A \cdot \left(\vec{P} - \vec{P}_A\right) = 0. \tag{63}$$

Expanding and rearranging,

$$a_{NA}x + b_{NA}y + c_{NA}z = d_{NA}, \tag{64}$$

where

$$d_{NA} = a_{NA}x_{A1} + b_{NA}y_{A1} + c_{NA}z_{A1}. \tag{65}$$

In Step 4 the foregoing procedure executed to calculate the equation of the plane through the center of cylinder B with an orientation so that $\vec{C}$ lies in the plane. The normal to this plane $\vec{N}_B$ is given by

$$\vec{N}_B = \vec{B} \times \vec{C} = a_{NB}\hat{i} + b_{NB}\hat{j} + c_{NB}\hat{k}, \tag{66}$$

where

$$\begin{aligned} a_{NB} &= b_B c_C - c_B b_C \\ b_{NB} &= c_B a_C - a_B c_C \\ c_{NB} &= a_B b_C - b_B a_C \end{aligned}. \tag{67}$$

The equation of the plane is given by the dot product of $\vec{N}_B$ and a vector in the plane from the point $P_B\left(x_{B1}, y_{B1}, z_{B1}\right)$ at the base of $\vec{B}$ and another point $P\left(x, y, z\right)$ in the plane so that

$$\vec{N}_B \cdot \left(\vec{P} - \vec{P}_B\right) = 0. \tag{68}$$

Expanding and rearranging,

$$a_{NB}x + b_{NB}y + c_{NB}z = d_{NB}, \tag{69}$$

where

$$d_{NB} = a_{NB}x_{B1} + b_{NB}y_{B1} + c_{NB}z_{B1}. \tag{70}$$

In Step 5 the parametric equations of the line L_I that is parallel to $\vec{C}$ and is through the intersection of the two planes are determined. These parametric equations are (Tierney, p 438)

$$\begin{aligned} L_I(t): x &= x_I + a_C t \\ y &= y_I + b_C t \\ z &= z_I + c_C t \end{aligned} \tag{71}$$

Line L_I is normal to and passes through the centers of cylinders A and B.

The intersection point (x_I, y_I, z_I) is determined by stipulating either *x*, *y*, or *z* and substituting into the two plane equations Eq.(64) and (69). This gives two equations of lines, the simultaneous solution of which gives a point. When either of the cylinders is oriented so that its axis is not parallel to any coordinate axis, then either *x*, *y*, or *z* can be stipulated. We arbitrarily select

$$z = z_I, \tag{72}$$

so that Eqs.(64) and (69) become

$$a_{NA}x + b_{NA}y + c_{NA}z_I = d_{NA}, \tag{73}$$

and

$$a_{NB}x + b_{NB}y + c_{NB}z_I = d_{NB}. \tag{74}$$

The simultaneous solution of Eqs.(73) and (74) gives

$$x_I = \frac{b_{NB}\left(d_{NA} - c_{NA}z_I\right) - b_{NA}\left(d_{NB} - c_{NB}z_I\right)}{a_{NA}b_{NB} - b_{NA}a_{NB}}, \tag{75}$$

and

$$y_I = \frac{d_{NB} - c_{NB}z_I - a_{NB}x_I}{b_{NB}}. \tag{76}$$

When each of the cylinders is parallel to a coordinate axis, the line L_I parallel to $\vec{C}$ is parallel to a coordinate axis. The stipulation of *x*, *y*, or *z* and subsequent substitution into the two plane equations Eq.(64) and (69) is made according to whether $\vec{C}$ is parallel to the *x*-, *y*-, or *z*-axis. For these cases, x_I is stipulated and y_I, z_I are solved for, y_I is stipulated and x_I, z_I are solved for, or z_I is stipulated and x_I, y_I are solved for as in Eqs.(75) and (76), respectively. The stipulated values of x_I, y_I or z_I are arbitrary.

Step 6 concerns the simultaneous solution of the equations for the surface cylinder A and the line L_I for the two points-of-intersections $\mathrm{POI}_{\mathrm{A1}}$ and $\mathrm{POI}_{\mathrm{A2}}$. This is done by inserting the expressions in Eq.(71) into Eq.(53) so that

$$a_{qA}t^2 + b_{qA}t + c_{qA} = 0, \tag{77}$$

where

$$
\begin{aligned}
a_{qA} &= a_C^2 A_A + b_C^2 B_A + c_C^2 C_A + a_c b_c D_A + b_C c_C E_A + a_C c_C F_A \\
b_{qA} &= \left(2a_C A_A + b_C D_A + c_C F_A\right) x_I + \left(2b_C B_A + a_C D_A + c_C E_A\right) y_I \\
&\quad + \left(2c_C C_A + b_C E_A + a_C F_A\right) z_I + a_C G_A + b_C H_A + c_C J_A \quad . \qquad (78) \\
c_{qA} &= A_A x_I^2 + B_A xy + C_A z_I^2 + D_A x_I y_I + E_A y_I z_I + F_A x_I z_I \\
&\quad + G_A x_I + H_A y_I + J_A z_I + K_A
\end{aligned}
$$

The quadratic expression in *t* given in Eq.(77) is solved for the two values t_{A1} and t_{A2},

$$
t_{A1} = \frac{-b_{qA} + \sqrt{b_{qA}^2 - 4a_{qA}c_{qA}}}{2a_{qA}}, t_{A1} = \frac{-b_{qA} - \sqrt{b_{qA}^2 - 4a_{qA}c_{qA}}}{2a_{qA}}. \qquad (79)
$$

The values t_{A1} and t_{A2} are the values of *t* for which L_I intersects cylinder A. Substitution of t_{A1} and t_{A2} into Eq.(71) gives the two POIs (x_{A1}, y_{A1}, z_{A1}) and (x_{A2}, y_{A2}, z_{A2}) on cylinder A,

$$
\begin{aligned}
x_{A1} &= x_0 + at_{A1} \\
y_{A1} &= y_0 + bt_{A1}\,, \qquad (80) \\
z_{A1} &= z_0 + ct_{A1}
\end{aligned}
$$

and

$$
\begin{aligned}
x_{A2} &= x_0 + at_{A2} \\
y_{A2} &= y_0 + bt_{A2}\,. \qquad (81) \\
z_{A2} &= z_0 + ct_{A2}
\end{aligned}
$$

The process is repeated for cylinder B whereby insertion of the expressions in Eq.(71) into Eq.(54) gives

$$
a_{qB}t^2 + b_{qB}t + c_{qB} = 0\,, \qquad (82)
$$

where

$$
\begin{aligned}
a_{qB} &= a_C^2 A_B + b_C^2 B_B + c_C^2 C_B + a_C b_C D_B + b_C c_C E_B + a_C c_C F_B \\
b_{qB} &= \left(2a_C A_B + b_C D_B + c_C F_B\right) x_I + \left(2b_C B_B + a_C D_B + c_C E_B\right) y_I \\
&\quad + \left(2c_C C_B + b_C E_B + a_C F_B\right) z_I + a_C G_B + b_C H_B + c_C J_B \quad . \qquad (83) \\
c_{qB} &= A_B x_I^2 + B_B xy + C_B z_I^2 + D_B x_I y_I + E_B y_I z_I + F_B x_I z_I \\
&\quad + G_B x_I + H_B y_I + J_B z_I + K_B
\end{aligned}
$$

The quadratic expression in *t* given in Eq.(77) is solved for the two values t_{B1} and t_{B1} to give

$$t_{B1} = \frac{-b_{qB} + \sqrt{b_{qB}^2 - 4a_{qB}c_{qB}}}{2a_{qB}}, t_{B1} = \frac{-b_{qB} - \sqrt{b_{qB}^2 - 4a_{qB}c_{qB}}}{2a_{qB}}. \tag{84}$$

The values t_{B1} and t_{B1} are the values of *t* for which L_I intersects cylinder B. Substitution of t_{B1} and t_{B1} into Eq.(71) gives the two POIs (x_{B1}, y_{B1}, z_{B1}) and (x_{B2}, y_{B2}, z_{B2}) for cylinder B,

$$\begin{aligned} x_{B1} &= x_0 + at_{B1} \\ y_{B1} &= y_0 + bt_{B1}, \\ z_{B1} &= z_0 + ct_{B1} \end{aligned} \tag{85}$$

and

$$\begin{aligned} x_{B2} &= x_0 + at_{B2} \\ y_{B2} &= y_0 + bt_{B2}. \\ z_{B2} &= z_0 + ct_{B2} \end{aligned} \tag{86}$$

In Step 8 a check is made to determine whether either the points of intersection POI_{A1} or POI_{A2} for cylinder A is in cylinder B. To do so, an assessment of the relative values of the parameter *t* is made. Consider Fig. 11.

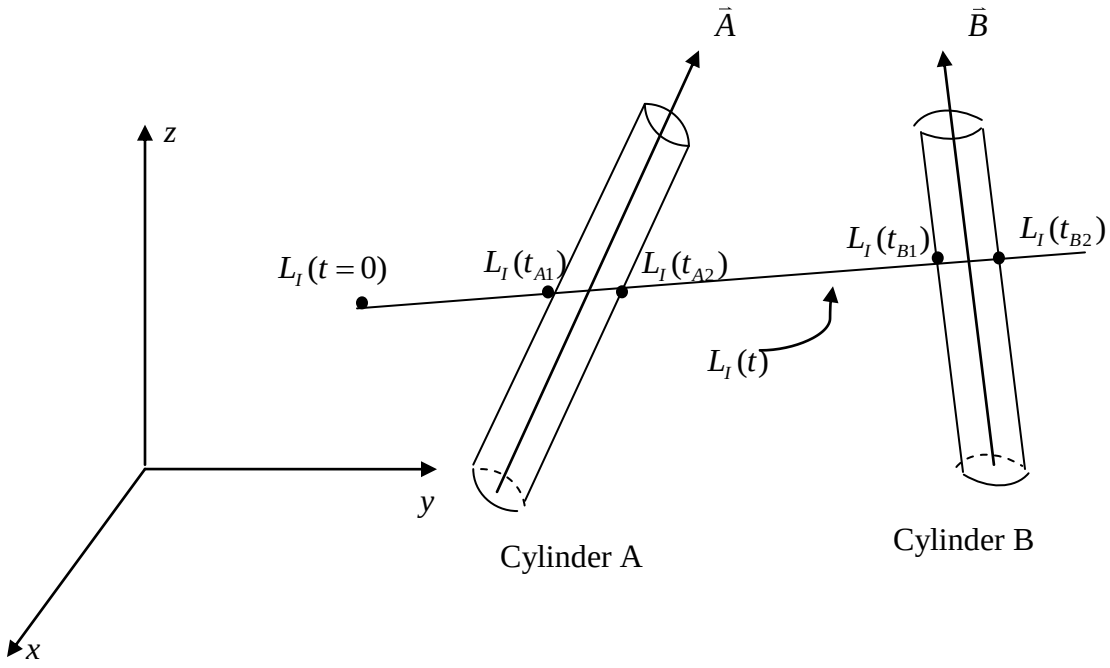

Figure 11. Two non-intersecting cylinders.

Cylinders A and B do not intersect when the following conditions are met:

$$\begin{aligned} &t_{A1} < t_{B1}, t_{A2} < t_{B1}; \\ &t_{A1} < t_{B2}, t_{A2} < t_{B2}. \end{aligned} \tag{87}$$

Cylinders A and B intersect when some combination of parameters exists such that a parameter for cylinder B is less than a parameter of cylinder A, e.g.,

$$t_{A1} < t_{B1} < t_{B2} < t_{A2}\,. \tag{88}$$

In Step 8 we note that because the cylindrical surfaces are infinite in extent, when two cylinders are found to intersect a determination must be made as to whether the intersection

occurs between the ends of the RCCs. The parameter values $t_{A1}, t_{A2}, t_{B1}, t_{B2}$ for the POIs created by the line L_l through radial center of cylinders A and B and the axis vectors $\vec{A}$ and $\vec{B}$ are known. Consequently, parametric equations of lines through these POIs in the directions of $\vec{A}$ and $\vec{B}$ can be written. The intersection of these lines with the planes at the ends of the cylinders can be calculated. An assessment as to whether the POIs are between the ends of the cylinders can then be made by consideration of the parameters for the lines.

The procedure is illustrated in Fig. 12.

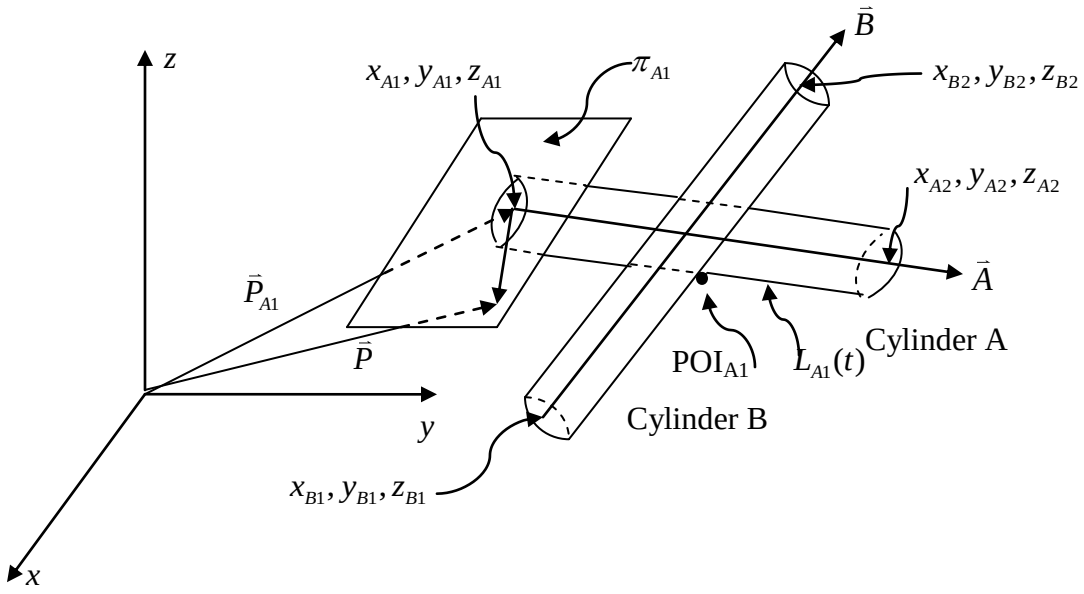

Figure 12. Determination whether POI_{A1} lies between the ends of RCCs A and B.

Consider the parameteric equations of the line $L_{A1}(t)$ through POI_{A1} in the direction of $\vec{A}$,

$$\begin{aligned} L_{A1}(t): x &= x(t_{A1}) + a_A t \\ y &= y(t_{A1}) + b_A t \,. \\ z &= z(t_{A1}) + c_A t \end{aligned} \tag{89}$$

The equation of the plane π_{A1} defining the end of RCC A through (x_{A1}, y_{A1}, z_{A1}) with normal $\vec{A}$ is

$$\pi_{A1} : \vec{A} \cdot \left(\vec{P} - \vec{P}_{A1} \right) = 0 , \tag{90}$$

where

$$\vec{P} = x\hat{i} + y\hat{j} + z\hat{k} , \tag{91}$$

and

$$\vec{P}_{A1} = x_{A1}\hat{i} + y_{A1}\hat{j} + z_{A1}\hat{k} . \tag{92}$$

Expanding and rearranging,

$$a_A x + b_A y + c_A z = d_{A1} , \tag{93}$$

where

$$d_{A1} = a_A x_{A1} + b_A y_{A1} + c_A z_{A1} . \tag{94}$$

Now solve Eqs.(89) and (93) simultaneously so that

$$t \equiv t_{A1A1} = \frac{d_{A1} - \left[a_A x\left(t_{A1}\right) + b_A y\left(t_{A1}\right) + c_A z\left(t_{A1}\right) \right]}{a_A^2 + b_A^2 + c_A^2} . \tag{95}$$

At the other plane for cylinder A, the equation of the plane through (x_{A2}, y_{A2}, z_{A2}) with normal $\vec{A}$ is that

$$\vec{A} \cdot \left(\vec{P} - \vec{P}_{A2} \right) = 0 , \tag{96}$$

where

$$\vec{P} = x\hat{i} + y\hat{j} + z\hat{k} , \tag{97}$$

and

$$\vec{P}_{A2} = x_{A2}\hat{i} + y_{A2}\hat{j} + z_{A2}\hat{k} . \tag{98}$$

Expanding and rearranging,

$$a_A x + b_A y + c_A z = d_{A2} , \tag{99}$$

where

$$d_{A2} = a_A x_{A2} + b_A y_{A2} + c_A z_{A2} . \tag{100}$$

Now solve Eqs.(89) and (99) simultaneously to obtain

$$t \equiv t_{A1A2} = \frac{d_{A2} - \left[a_A x\left(t_{A1}\right) + b_A y\left(t_{A1}\right) + c_A z\left(t_{A1}\right) \right]}{a_A^2 + b_A^2 + c_A^2} . \tag{101}$$

The condition that $\mathrm{POI}_{\mathrm{A1}}$ lies between the ends of RCC A is

$$t_{A1A1} < t_{A1} < t_{A1A2} . \tag{102}$$

If this condition is satisified, then the two RCCs intersect. If it is not satisfied, then the procedure is repeated for $\mathrm{POI}_{\mathrm{A2}}$.

For $\mathrm{POI}_{\mathrm{A2}}$, the parameteric equations of the line $L_{A2}(t)$ through $\mathrm{POI}_{\mathrm{A2}}$ in the direction of $\bar{A}$ are

$$\begin{aligned} L_{A2}(t): x &= x\left(t_{A2}\right) + a_A t \\ y &= y\left(t_{A2}\right) + b_A t . \\ z &= z\left(t_{A2}\right) + c_A t \end{aligned} \tag{103}$$

The simultaneous solution of Eqs.(93) and (103) gives

$$t \equiv t_{A2A1} = \frac{d_{A1} - \left[a_A x\left(t_{A2}\right) + b_A y\left(t_{A2}\right) + c_A z\left(t_{A2}\right) \right]}{a_A^2 + b_A^2 + c_A^2} . \tag{104}$$

The simultaneous solution of Eqs.(99) and (103) gives

$$t \equiv t_{A2A2} = \frac{d_{A2} - \left[a_A x\left(t_{A2}\right) + b_A y\left(t_{A2}\right) + c_A z\left(t_{A2}\right) \right]}{a_A^2 + b_A^2 + c_A^2} . \tag{105}$$

The condition that $\mathrm{POI}_{\mathrm{A2}}$ lies between the ends of RCC A is

$$t_{A2A1} < t_{A2} < t_{A2A2} . \tag{106}$$

If this condition is satisified, then the two RCCs intersect. If it is not satisfied, then the cylindrical sides of RCCs A and B do not intersect. If a non-intersection finding is made, then a check must be made to determine whether the ends of the RCCs intersect.

Step 9 considers the situation where the ends of the RCCs intersect. Four cases of intersections are possible: (1) top of RCC A and top of RCC B, (2) top of RCC A and bottom of RCC B, (3) bottom of RCC A and top of RCC B, and (4) bottom of RCC A and bottom of RCC B. Fig. 13 illustrates the case where RCC B penetrates the top planar surface of RCC A without intersecting the wall of RCC A.

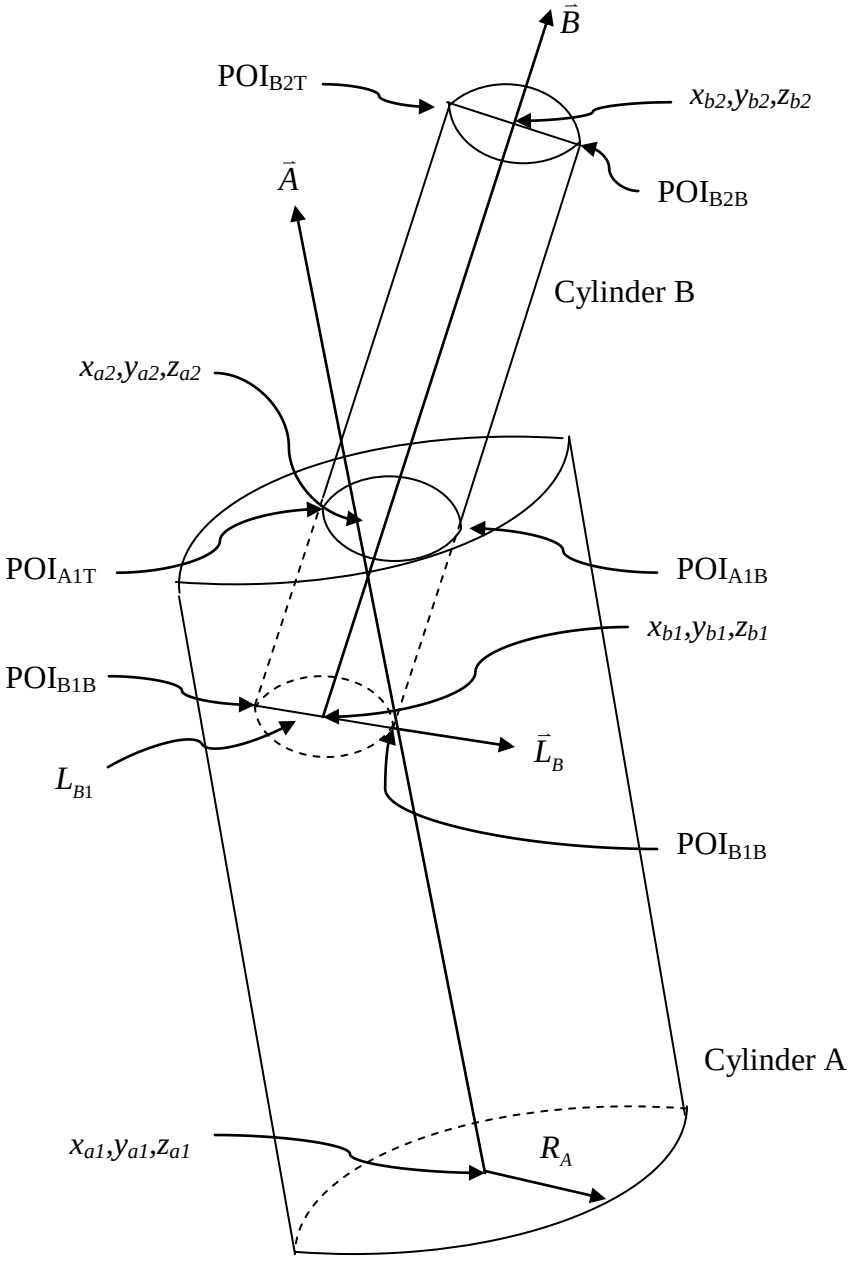

Figure 13. RCC B intersecting the top end of RCC A.

This assessments begins by calculating the equation of the plane π_{AB} through $\vec{A}$ and $\vec{B}$, vectors through (x_{A1}, y_{A1}, z_{A1}) and (x_{A2}, y_{A2}, z_{A2}), respectively, and parallel to the axes of the cylinders. This equation is given in terms of dot product of the normal $\vec{C}$ to the plane, given by the cross product of $\vec{A}$ and $\vec{B}$, and a vector in the plane. The vector in π_{AB} is written in terms of a point $P(x, y, z)$ and any point along $\vec{A}$, so the point $P_{A1}(x_{A1}, y_{A1}, z_{A1})$ is selected. Then

$$\pi_{AB} : \vec{C} \cdot \left(\vec{P} - \vec{P}_{A1} \right) = 0, \tag{107}$$

or

$$a_C x + b_C y + c_C z = d_C, \tag{108}$$

with

$$d_C = a_C x_{A1} + b_C y_{A1} + c_C z_{A1}. \tag{109}$$

Next, the plane π_{B1} on the bottom of RCC B is

$$\pi_{B1} : \vec{B} \cdot \left(\vec{P} - \vec{P}_{B1} \right) = 0, \tag{110}$$

so that

$$a_B x + b_B y + c_B z = d_{B1}, \tag{111}$$

with

$$d_{B1} = a_B x_{B1} + b_B y_{B1} + c_B z_{B1}. \tag{112}$$

The intersection of planes π_{AB} and π_{B1} is a line. The parametric equations of this line, L_{B1}, are specified using a point on this line which is conveniently selected to be the point at the base and on the axis of RCC B, $P_{B1}(x_{B1}, y_{B1}, z_{B1})$. The direction of line L_{B1} is perpendicular to the normals to π_{AB} and π_{B1}. So,

$$\vec{L}_B = \vec{B} \times \vec{C} = a_{LB} \hat{i} + b_{LB} \hat{j} + c_{LB} \hat{k}, \tag{113}$$

where

$$\begin{aligned} a_{LB} &= b_B c_C - c_B b_C \\ b_{LB} &= c_B a_C - a_B c_C \\ c_{LB} &= a_B b_C - b_B a_C \end{aligned} . \qquad (114)$$

The parametric equations for the line $L_{B1}(t)$ are

$$\begin{aligned} L_{B1}(t): x &= x_{B1} + a_{LB} t \\ y &= y_{B1} + b_{LB} t \\ z &= z_{B1} + c_{LB} t \end{aligned} . \qquad (115)$$

A calculation is now made for the two POIs at the intersection of $L_{B1}(t)$ and RCC B, POI_{B1T} (for "top") and POI_{B1B} (for "bottom"). The designators "top" and "bottom" are used for convenience – in essence, two values are calculated. Substituting the expressions in Eq.(115) into Eq.(53) gives the quadratic

$$a_{qLB1} t^2 + b_{qLB1} t + c_{qLB1} = 0, \qquad (116)$$

with the coefficients

$$\begin{aligned} a_{qLB1} &= a_{LB}^2 A_B + b_{LB}^2 B_B + c_{LB}^2 C_B + a_{LB} b_{LB} D_B + b_{LB} c_{LB} E_B + a_{LB} c_{LB} F_B \\ b_{qLB1} &= \left(2 a_{LB} A_B + b_{LB} D_B + c_{LB} F_B\right) x_{B1} + \left(2 b_{LB} B_B + a_{LB} D_B + c_{LB} E_B\right) y_{B1} \\ &\quad + \left(2 c_{LB} C_B + b_{LB} E_B + a_{LB} F_B\right) z_{B1} + a_{LB} G_B + b_{LB} H_B + c_{LB} J_B \\ c_{qLB1} &= A_B x_{B1}^2 + B_B xy + C_B z_{B1}^2 + D_B x_{B1} y_{B1} + E_B y_{B1} z_{B1} + F_B x_{B1} z_{B1} \\ &\quad + G_B x_{B1} + H_B y_{B1} + J_B z_{B1} + K_B \end{aligned} . \qquad (117)$$

The quadratic expression in *t* given in Eq.(116) is solved for the two values t_{LB1-1} and t_{LB1-2},

$$t_{LB1-1} = \frac{-b_{qLB1} + \sqrt{b_{qLB1}^2 - 4 a_{qLB1} c_{qLB1}}}{2 a_{qLB1}}, t_{LB1-2} = \frac{-b_{qLB1} - \sqrt{b_{qLB1}^2 - 4 a_{qLB1} c_{qLB1}}}{2 a_{qLB1}} . \qquad (118)$$

The parametric equation of the lines through POI_{B1T} and POI_{B1B} in the direction $\bar{B}$ are then given by

$$\begin{aligned} L_{B1T}(t): x &= x_{LB1-1} + a_B t \\ y &= y_{LB1-1} + b_B t \\ z &= z_{LB1-1} + c_B t \end{aligned} \tag{119}$$

and

$$\begin{aligned} L_{B1B}(t): x &= x_{LB1-2} + a_B t \\ y &= y_{LB1-2} + b_B t \\ z &= z_{LB1-2} + c_B t \end{aligned} . \tag{120}$$

The parametric equations of the lines in Eqs.(119) and (120) are solved simultaneously with the equations of planes π_{A1} and π_{A2} through the bottom and top of RCC A. For π_{A1}, using Eqs.(90)–(94) and Eq.(119) gives

$$t \equiv t_{LB1-1-A1} = \frac{d_{A1} - \left[a_A x\left(t_{LB1-1}\right) + b_A y\left(t_{LB1-1}\right) + c_A z\left(t_{LB1-1}\right) \right]}{a_A a_B + b_A b_B + c_A c_B} , \tag{121}$$

while Eq.(120) gives

$$t \equiv t_{LB1-2-A1} = \frac{d_{A1} - \left[a_A x\left(t_{LB1-2}\right) + b_A y\left(t_{LB1-2}\right) + c_A z\left(t_{LB1-2}\right) \right]}{a_A a_B + b_A b_B + c_A c_B} . \tag{122}$$

For π_{A2}, using Eqs.(90)–(94) and Eq.(119) gives

$$t \equiv t_{LB1-1-A2} = \frac{d_{A2} - \left[a_A x\left(t_{LB1-1}\right) + b_A y\left(t_{LB1-1}\right) + c_A z\left(t_{LB1-1}\right) \right]}{a_A a_B + b_A b_B + c_A c_B} , \tag{123}$$

while Eq.(120) gives

$$t \equiv t_{LB1-2-A2} = \frac{d_{A2} - \left[a_A x\left(t_{LB1-2}\right) + b_A y\left(t_{LB1-2}\right) + c_A z\left(t_{LB1-2}\right) \right]}{a_A a_B + b_A b_B + c_A c_B} . \tag{124}$$

Next, a check is made to determine whether the POIs lie within the axial limits of RCC B. This is done by assessing the intersection of RCC B with the planes π_{A1} and π_{A2} at the lower and upper extremities, respectively, of RCC A. The procedure is clarified by the diagrams in Figs.14 and 15, which show a cross-section of RCC A in plane π_{A1}. The intersection of RCC B with plane π_{A1} can produce a circle, if the axes of RCC A and B are parallel, or an ellipse if the axes of RCC A and B are not parallel. The intersecting surface can be contained entirely within RCC A, or could be partially enclosed in RCC A.

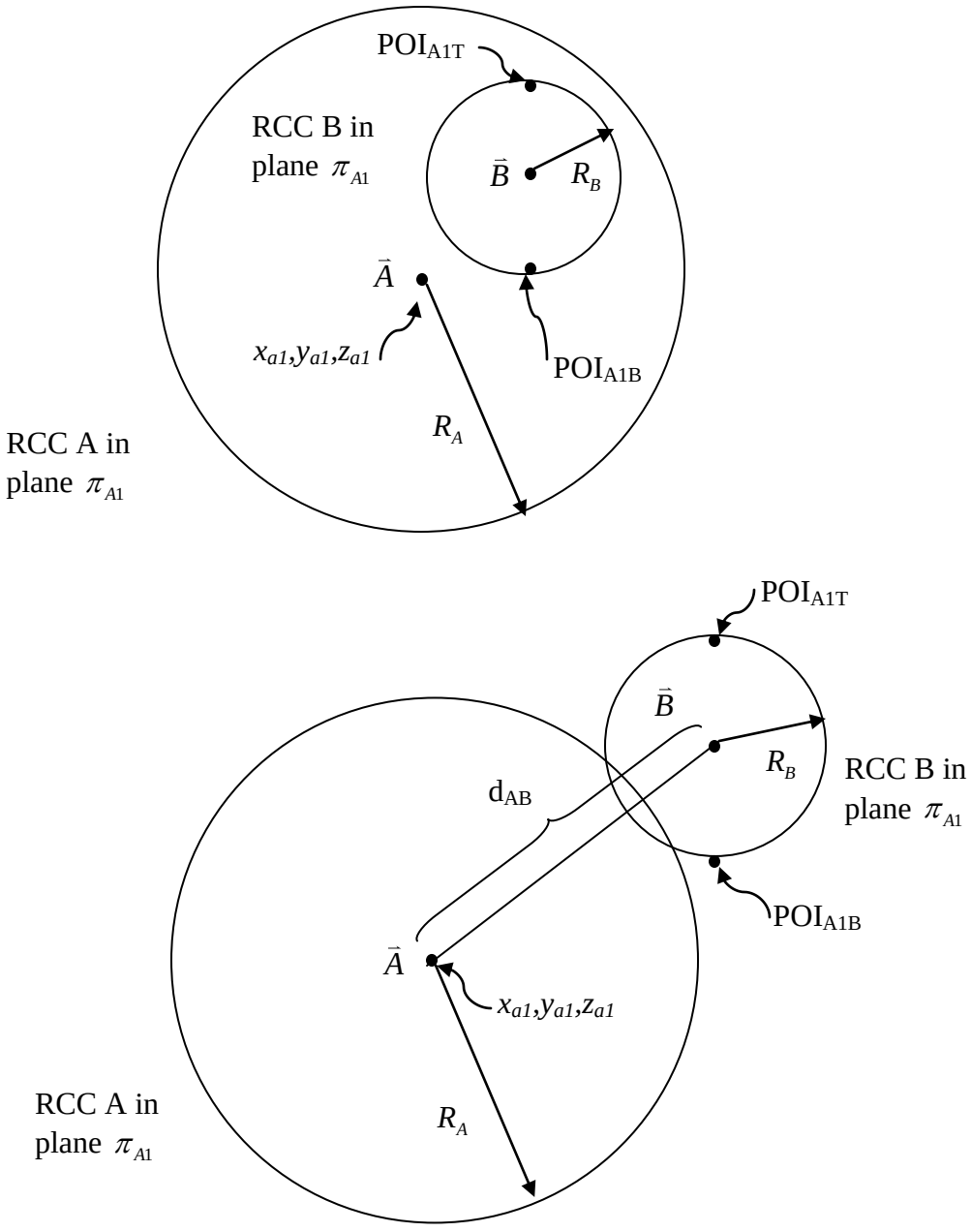

Figure 14. RCC B intersecting the base of RCC A for axes $\vec{A}$ and $\vec{B}$ parallel and out of plane π_{A1}. Upper: complete intersection. Lower: Partial intersection with POI$_{A1T}$ and POI$_{A1B}$ out of RCC A.

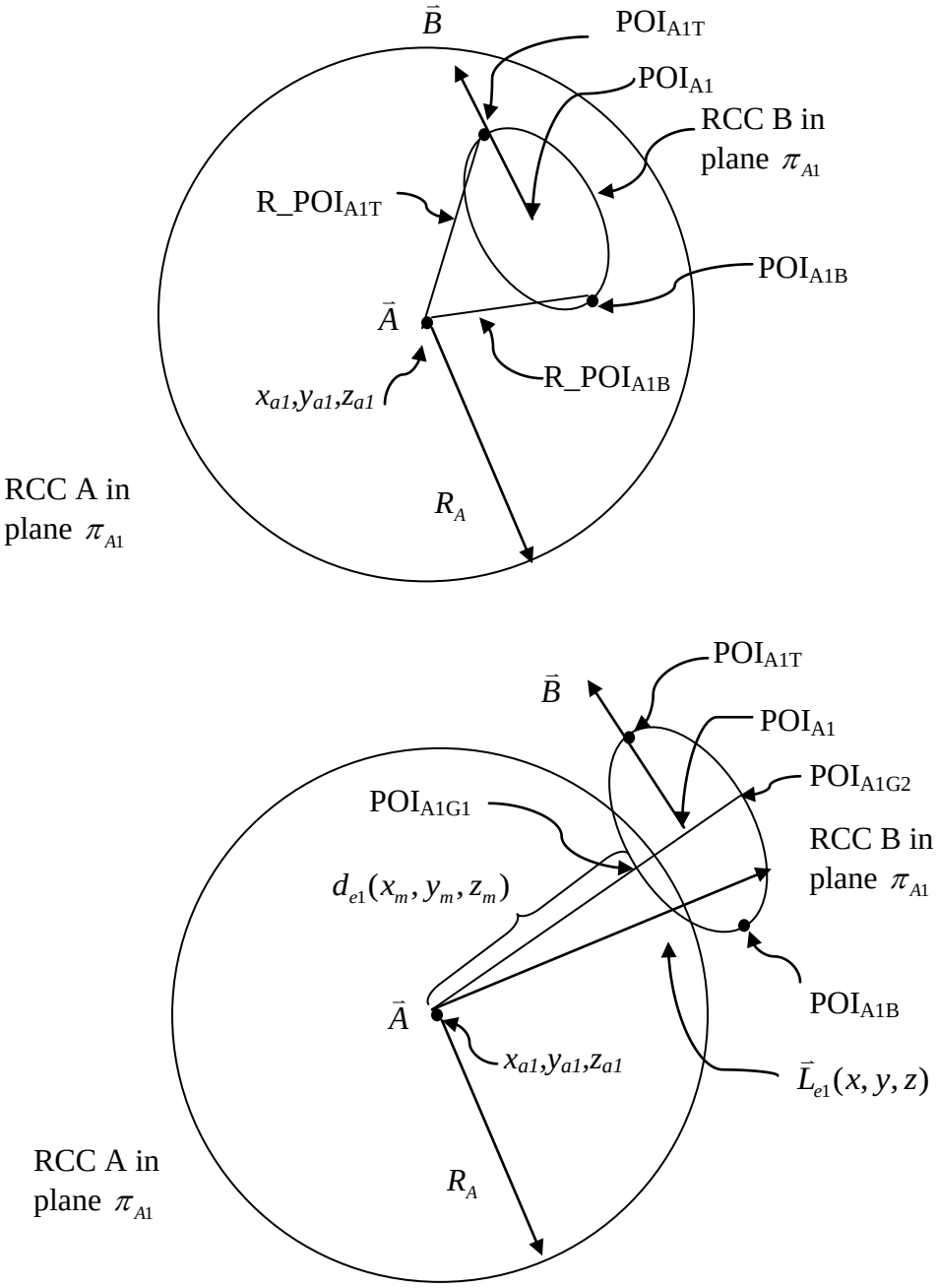

Figure 15. RCC B intersecting the base of RCC A for axes $\vec{A}$ and $\vec{B}$ not parallel and out of plane π_{A1}. Upper: complete intersection. Lower: Partial intersection with POI$_{A1T}$ and POI$_{A1B}$ out of RCC A.

For the case where the axes of RCCs A and B are parallel, determination as to whether intersection occurs can be made by comparing the radii of RCCs A and B, R_A and R_B, and the distance d_{AB} from the center of RCC A in plane π_{A1} to the point of intersection POI_{A1M} at the center of RCC B with plane π_{A1}. POI_{A1M} is given by the intersection of the line $L_B(t)$ parallel to $\vec{B}$ through the center of RCC B and plane π_{A1}. The parametric equations for the line $L_B(t)$ are

$$\begin{aligned} L_B(t): x &= x_{B1} + a_B t \\ y &= y_{B1} + b_B t \,. \\ z &= z_{B1} + c_B t \end{aligned} \tag{125}$$

Substitution of these expressions into the equation of plane π_{A1} given in Eq.(93) and solving for *t* gives

$$t \equiv t_M = \frac{-\left(a_A x_{B1} + b_A y_{B1} + c_A z_{B1}\right)}{a_A a_B + b_A b_B + c_A c_B} \,. \tag{126}$$

The distance d_{AB} is thus

$$d_{AB} = \left\{ \left[x_{A1} - x\left(t_M\right) \right]^2 + \left[y_{A1} - y\left(t_M\right) \right]^2 + \left[z_{A1} - z\left(t_M\right) \right]^2 \right\} \tag{127}$$

Intersection of RCCs A and B occurs when

$$d_{AB} < R_A + R_B \,. \tag{128}$$

Assessment of the intersection when the axes of RCC A and B are not parallel is more complicated because the orientation of the ellipse in plane π_{A1} depends on the orientation of RCC B. The assessment is done in two stages.

In Stage 1, checks are made to determine whether either the "top" or "bottom" intersection points of RCC B with RCC A plane π_{A1}, R_POI_{A1T} or R_POI_{A1B}, lie inside RCC A. Thus,

$$\begin{aligned} R\_POI_{A1T} &< R_A \\ R\_POI_{A1B} &< R_A \end{aligned}. \tag{129}$$

If either condition is satisfied, then RCCs A and B intersect.

If neither condition is satisfied, then a more complicated intersection check is necessary for Stage 2. This situation is illustrated in Fig.12 for the case where the intersection of RCC B with plane π_{A1} creates an ellipse that may partially intersect RCC A. Here, an intersection assessment can be made by determining the minimal distance between the center of RCC A in plane π_{A1}, (x_{A1}, y_{A1}, z_{A1}), and the ellipse. To do so, the method of Lagrange multipliers (Trench and Kolman, 1972) is used to do the analysis. Using this technique, the distance d_{e1} between the center of RCC A in plane π_{A1}, (x_{A1}, y_{A1}, z_{A1}), and the intersection of the cylinder with plane π_{A1}, i.e., the ellipse, is minimized. It is convenient to use the distance measure[1]

$$f(x,y,z) = d_{e1}^2 = (x - x_{A1})^2 + (y - y_{A1})^2 + (z - z_{A1})^2, \tag{130}$$

where $f(x,y,z)$ is termed the objective function.

[1] This form simplifies the analysis as compared to using $f(x,y,z) = d_{e1}$.

This distance is minimized subject to two constraints. Constraint 1 is that all values (x, y, z) must lie on the surface of the general cylinder given by Eq.(54) and written here as $g_1(x, y, z)$, where

$$g_1(x, y, z) \equiv A_B x^2 + B_B y^2 + C_B z^2 + D_B xy + E_B yz + F_B zx + G_B x + H_B y + J_B z + K_B = 0 \text{ .(131)}$$

Constraint 2 requires that all values (x, y, z) lie on the line designated by the vector $\hat{L}_{e1}$ originating at the center of RCC A in plane π_{A1}, (x_{A1}, y_{A1}, z_{A1}), and oriented in the plane π_{A1}. Thus,

$$\vec{L}_{e1} = (x - x_{A1})\hat{i} + (y - y_{A1})\hat{j} + (z - z_{A1})\hat{k} \,. \qquad (132)$$

This constraint is needed to ensure that the minimial distance is between calculated in the plane π_{A1}.[2] Vector $\hat{L}_{e1}$ must be perpendicular to the normal $\vec{A}$ of the plane π_{A1} so that Constraint 2 $g_2(x, y, z)$ is

$$g_2(x, y, z) \equiv \vec{A} \cdot \vec{L}_{e1} = 0 \,, \qquad (133)$$

or

$$g_2(x, y, z) \equiv a_A (x - x_{A1}) + b_A (y - y_{A1}) + c_A (z - z_{A1}) = 0 \,, \qquad (134)$$

or

$$g_2(x, y, z) = a_A x + b_A y + c_A z - d_{A1} = 0 \,. \qquad (135)$$

[2] Consider RCC A to be a quarter and RCC B to be a toothpick which slightly penetrates the quarter near the outer periphery of the quarter. RCC B might be oriented almost parallel to the bottom of the quarter so that the minimum distance between the center of the quarter and the toothpick is much less than the distance from the center of the quarter to the location of intersection of the quarter and toothpick.

The Lagrange multiplier formulation can be simplified by first solving Eq. (134) for *z* so that

$$z(x,y)=\frac{\left[d_{A1}-\left(a_A x-b_A y\right)\right]}{c_A}. \tag{136}$$

The analysis proceeds using bivariate expressions in the independent variables *x* and *y*.

An auxiliary function F is formed using the objective function in Eq.(130), the explicit constraint in Eq.(131) and the implicit constraint in Eq.(136), and the Lagrange multiplier λ so that

$$F\left(x,y\right)=f\left(x,y\right)+\lambda g\left(x,y\right). \tag{137}$$

The conditions to be satisfied are

$$\begin{aligned}\frac{\partial F}{\partial x}&=\frac{\partial f}{\partial x}+\lambda\frac{\partial g}{\partial x}=0\\ \frac{\partial F}{\partial y}&=\frac{\partial f}{\partial y}+\lambda\frac{\partial g}{\partial y}=0\end{aligned}. \tag{138}$$

Solving the expressions in Eq.(138) yields

$$\frac{\partial f}{\partial x}\frac{\partial g}{\partial y}-\frac{\partial f}{\partial y}\frac{\partial g}{\partial x}=0. \tag{139}$$

Evaluation of the partial derivatives gives

$$\begin{aligned}\frac{\partial f}{\partial x}&=2\left(x-x_{A1}\right)+2\left(z-z_{A1}\right)\frac{\partial z}{\partial x}\\ \frac{\partial f}{\partial y}&=2\left(y-y_{A1}\right)+2\left(z-z_{A1}\right)\frac{\partial z}{\partial y}\end{aligned} \tag{140}$$

$$\frac{\partial g}{\partial x} = 2A_B x + 2C_B \frac{\partial z}{\partial x} + D_B y + E_B y \frac{\partial z}{\partial x} + F_B \left(\frac{\partial z}{\partial x} x + z \right) + G_B + J_B \frac{\partial z}{\partial x}$$
$$\frac{\partial g}{\partial y} = 2B_B y + 2C_B \frac{\partial z}{\partial y} + D_B x + E_B \left(z + y \frac{\partial z}{\partial y} \right) + F_B \frac{\partial z}{\partial y} x + H_B + J_B \frac{\partial z}{\partial y} \quad , \tag{141}$$

and

$$\frac{\partial z}{\partial x} = -\frac{a_A}{c_A}, \quad \frac{\partial z}{\partial y} = -\frac{b_A}{c_A} . \tag{142}$$

Inserting the expressions in Eqs.(141) and (142) into Eq.(139) gives

$$A_{BL} x^2 + B_{BL} y^2 D_{BL} xy + G_{BL} x + H_{BL} y + K_{BL} = 0 \tag{143}$$

where (Wolfram, 1991)

$$\begin{aligned}
A_{BL} &= 4A_B a_A b_A c_A + 2D_B \left(c_A^3 + a_A^2 c_A \right) - 2E_B \left(a_A^3 + a_A c_A^2 \right) + 2F_B \left(a_A^2 b_A - b_A c_A^2 \right) \\
B_{BL} &= 4B_B a_A b_A c_A - 2D_B \left(c_A^3 + b_A^2 c_A \right) + 2E_B \left(-a_A b_A^2 + a_A c_A^2 \right) + 2F_B \left(b_A^3 + b_A c_A^2 \right) \\
D_{BL} &= -4A_B \left(c_A^3 + b_A^2 c_A \right) + 4B_B \left(c_A^3 + a_A^2 c_A \right) - 4E_B \left(a_A^2 b_A + b_A c_A^2 \right) + 4F_B \left(a_A b_A^2 + a_A c_A^2 \right) \\
G_{BL} &= 4A_B \left(-b_A c_A^2 z_{A1} + b_A c_A d_{A1} \right) - 4C_B b_A c_A^2 + 2D_B \left(a_A c_A^2 z_{A1} - a_A c_A d_{A1} \right) \\
&\quad + E_B \left(-2a_A^2 c_A z_{A1} + 4a_A^2 d_{A1} + 2c_A^2 d_{A1} + 2a_A c_A^2 x_{A1} \right) \\
&\quad + F_B \left(2a_A b_A c_A z_{A1} - 4a_A b_A d_{A1} + 2b_A c_A^2 x_{A1} - a_A c_A^2 y_{A1} \right) \\
&\quad - 2G_B a_A b_A c_A + 2H_B \left(c_A^3 + a_A^2 c_A \right) - 2J_B b_A c_A^2 \\
H_{BL} &= 4B_B \left(a_A c_A^2 z_{A1} - a_A c_A d_{A1} \right) + 4C_B a_A c_A^2 + 2D_B \left(-b_A c_A^2 z_{A1} + b_A c_A d_{A1} \right) \\
&\quad + E_B \left(-2a_A b_A c_A z_{A1} + 4a_A b_A d_{A1} + 4b_A c_A^2 x_{A1} - 2a_A c_A^2 y_{A1} \right) \\
&\quad + F_B \left(2b_A^2 c_A z_{A1} - 4b_A^2 d_{A1} - 2c_A^2 d_{A1} - 2b_A c_A^2 y_{A1} \right) \\
&\quad - 2G_B \left(c_A^3 + b_A^2 c_A \right) + 2H_B a_A b_A c_A + 2J_B a_A c_A^2 \\
K_{BL} &= 4C_B \left(b_A c_A^2 x_{A1} - a_A c_A^2 y_{A1} \right) + 2E_B \left(a_A c_A d_{A1} z_{A1} - a_A d_{A1}^2 - c_A^2 d_{A1} x_{A1} \right) \\
&\quad + 2F_B \left(-b_A c_A d_{A1} z_{A1} + b_A d_{A1}^2 + c_A^2 d_{A1} y_{A1} \right) + 2G_B \left(-b_A c_A^2 z_{A1} + b_A c_A d_{A1} + c_A^3 y_{A1} \right) \\
&\quad + 2H_B \left(a_A c_A^2 z_{A1} - a_A c_A d_{A1} - c_A^3 x_{A1} \right) + 2J_B \left(b_A c_A^2 x_{A1} - a_A c_A^2 y_{A1} \right)
\end{aligned} \tag{144}$$

Equation (130), with Eq.(136), and Eq. (143) constitute two general quadratic equations in the unknowns x and y. In general, their simultaneous solution must be obtained using a multivariate root-finding algorithm.

If a POI is determined, then the procedure is terminated. If no POI is located, then the foregoing analysis is repeated for the upper end of RCC B, and then for the upper end of RCC A and the ends of RCC B.

3.5. RCC and SPH

The intersection of a cylinder and a sphere requires formulations and evaluation procedure that differs from those for the preceding types of intersections. It is necessary to treat three primary configurations characterized in terms of the location of the center of the sphere relative to the cylinder. Configuration 1 pertains to a sphere that is located such that its center lies between the axial extremities of the cylinder as illustrated in Fig. 16. Configurations 2 and 3, to be discussed later, consider the sphere when its center is beyond either end of the cylinder.

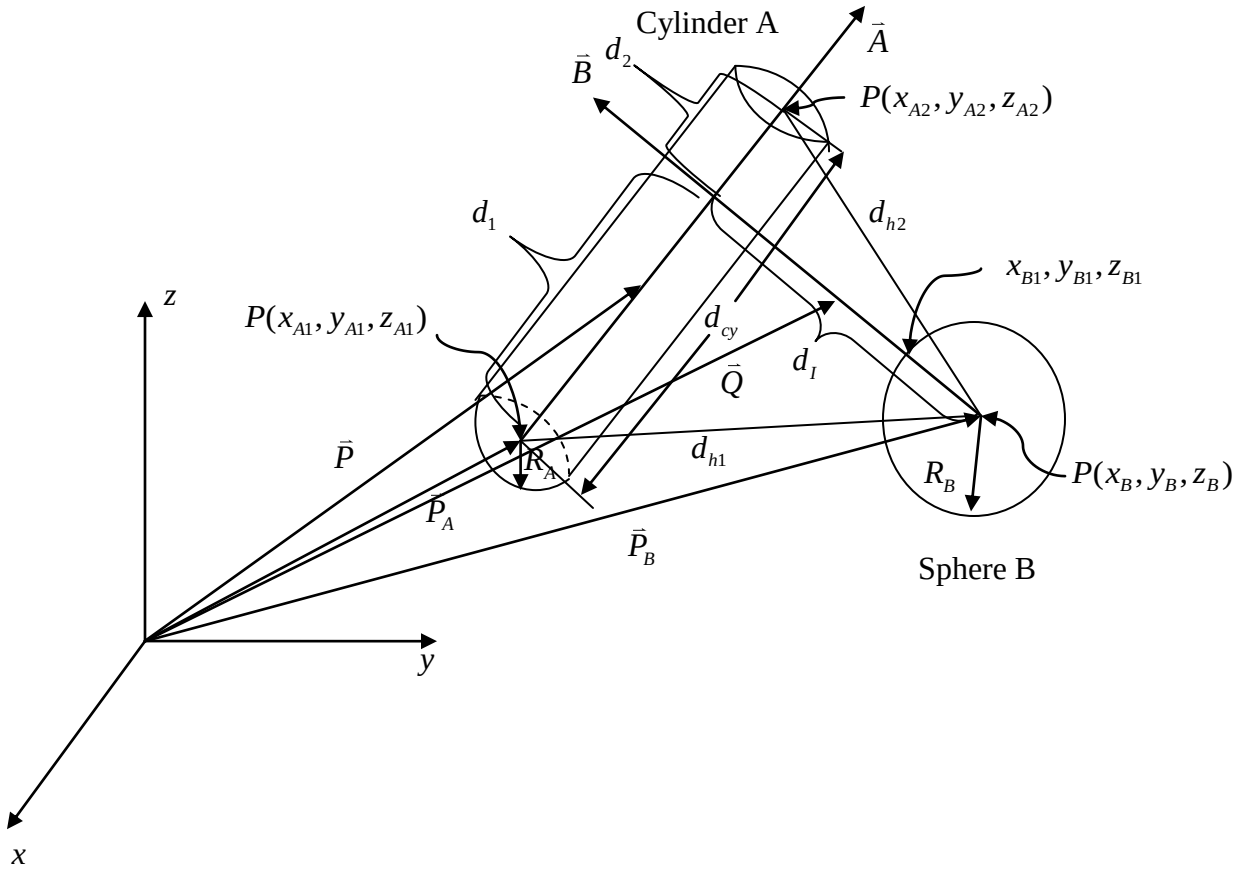

Figure 16. Collision of cylinder and sphere for Configuration 1.

The RCC-SPH PDS is:

1. Determine the vector $\vec{A}$ parallel to the axis of RCC A
2. Calculate the parametric equations of the line parallel to $\vec{A}$ through the base of the RCC.
3. Calculate the vector $\vec{B}$ from the center of SPH A orthogonal to $\vec{A}$.
4. Form the parametric equations for the line in the direction $\vec{B}$ through the center of SPH A.
5. Use trigonometry to determine the POI.

Configuration 1: sphere is inside of axial extremities of cylinder.

Referencing Fig. 16, consider a cylinder A with a base located at $P(x_{A1}, y_{A1}, z_{A1})$ as referenced by the vector $\vec{P}_A$ extending from the origin to (x_{A1}, y_{A1}, z_{A1}) The cylinder is oriented in the direction of vector $\vec{A}$, and has a radius R_A and length d_{cy} with terminal centerpoint located at $P(x_{A2}, y_{A2}, z_{A2})$. The vector $\vec{A}$ is given by

$$\vec{A} = a_A\hat{i} + b_A\hat{j} + c_A\hat{k}, \tag{145}$$

where

$$\begin{aligned} a_A &= x_{A2} - x_{A1} \\ b_A &= y_{A2} - y_{A1}. \\ c_A &= z_{A2} - z_{A1} \end{aligned} \tag{146}$$

A fixed point and a fixed direction characterize a line in three dimensions (Tierney, 1974). Thus, if the point $P(x_{A1}, y_{A1}, z_{A1})$ is a point on line L which has the direction of vector $\vec{A}$ and $P(x, y, z)$ is any point on L, there exists a scalar *t* such that

$$\vec{P} = \vec{P}_A + t\vec{A}. \tag{147}$$

Every vector equation is equivalent to three scalar equations, obtained by equating the components of both sides of the equation. Thus, Eq.(147) is equivalent to the three scalar equations

$$\begin{aligned} x &= x_{A1} + a_A t \\ y &= y_{A1} + b_A t. \\ z &= z_{A1} + c_A t \end{aligned} \tag{148}$$

These expressions are known as the parametric equations of L with *t* serving as the parameter.

Also consider a sphere B whose center is located at $P(x_B, y_B, z_B)$ as referenced by the vector $\vec{P}_B$ extending from the origin to (x_B, y_B, z_B). The sphere has a radius R_B.

To develop a cylinder-box PDS, we first construct a vector $\vec{B}$ extending from the center of the sphere through the center of the cylinder with a direction such that $\vec{B}$ is orthogonal to $\vec{A}$. The vector $\vec{B}$ is given as

$$\vec{B} = a_B\hat{i} + b_B\hat{j} + c_B\hat{k} \tag{149}$$

Similar to the discussion for $\vec{A}$, if the point $P(x_B, y_B, z_B)$ is a point on line M with the direction of vector $\vec{B}$ and $Q(x, y, z)$ is any point on M, there exists a scalar *u* such that

$$\vec{Q} = \vec{P}_B + u\vec{B}. \tag{150}$$

The equation of a line M in the direction $\vec{B}$ through the point $P(x_B, y_B, z_B)$ can be written in terms of the parameter *u* as

$$\begin{aligned} x &= x_B + a_B u \\ y &= y_B + b_B u \\ z &= z_B + c_B u \end{aligned}. \tag{151}$$

Lines L and M have the point of intersection (POI) at $P(x_I, y_I, z_I)$. The coordinates of this point permit us to write the coefficients of $\vec{B}$ as

$$\begin{aligned} a_B &= x_I - x_B \\ b_B &= y_I - y_B \\ c_B &= z_I - z_B \end{aligned}. \tag{152}$$

To determine the POI, it is convenient to develop trigonometric formulations. First, the quantity d_1 is defined as the distance between cylinder endpoint (x_{A1}, y_{A1}, z_{A1}) and the POI on the centerline of the cylinder. Similarly, d_2 is defined as the distance between (x_{A2}, y_{A2}, z_{A2}) and the POI. The total length of the cylinder can be written in terms of d_1 and d_2 as

$$d_{cy} = d_1 + d_2 = \left[\left(x_{A2} - x_{A1} \right)^2 + \left(y_{A2} - y_{A1} \right)^2 + \left(z_{A2} - z_{A1} \right)^2 \right]^{1/2}. \tag{153}$$

Second, the quantity d_{h1} is defined as the distance between the center of the sphere (x_B, y_B, z_B) and the endpoint (x_{A1}, y_{A1}, z_{A1}) on the centerline of the cylinder. Similarly, d_{h2} is defined as the distance between (x_B, y_B, z_B) and (x_{A2}, y_{A2}, z_{A2}). These distances are given as

$$\begin{aligned} d_{h1} &= \left[\left(x_{A1} - x_B \right)^2 + \left(y_{A1} - y_B \right)^2 + \left(z_{A1} - z_B \right)^2 \right]^{1/2} \\ d_{h2} &= \left[\left(x_{A2} - x_B \right)^2 + \left(y_{A2} - y_B \right)^2 + \left(z_{A2} - z_B \right)^2 \right]^{1/2} \end{aligned} \tag{154}$$

and are thus known values.

Third, use of the Pythagorean theorem yields the relationships

$$d_{h1}^2 = d_I^2 + d_1^2, \tag{155}$$

and

$$d_{h2}^2 = d_I^2 + d_2^2. \tag{156}$$

Fourth, Eqs.(155) and (156) are solved using Eq.(153). Solving Eq.(153) for d_2, substituting in Eq.(156), and solving the resulting expression and Eq.(155) simultaneously gives

$$d_1 = \frac{d_{h1}^2 - d_{h2}^2 + d_{cy}^2}{2 d_{cy}} \tag{157}$$

and

$$d_2 = d_{cy} - d_1 . \tag{158}$$

The value d_1 given by Eq.(157) corresponds to the parameter $t = t_I = d_I$, which can be used in Eq.(148) to give the POI (x_I, y_I, z_I).

A determination as to whether the sphere intersects the cylinder can now be made. First, the parametric equation of the line M along $\vec{B}$ given by Eq.(151) is evaluated using the coefficients in Eq.(152). Two values of the parameter *u* are selected,

$$\begin{aligned} u_1 &= R_B \\ u_2 &= -R_B \end{aligned} \tag{159}$$

so that the closest and furthest distances $d(R_B)$ and $d(-R_B)$ from the POI to the sphere along M are determined as

$$\begin{aligned} d(R_B) \equiv d_{B1} &= \left[\left(x_I - x_{B1} \right)^2 + \left(y_I - y_{B1} \right)^2 + \left(z_I - z_{B1} \right)^2 \right]^{1/2} \\ d(-R_B) \equiv d_{B2} &= \left[\left(x_I - x_{B2} \right)^2 + \left(y_I - y_{B2} \right)^2 + \left(z_I - z_{B2} \right)^2 \right]^{1/2} \end{aligned} \tag{160}$$

The criteria for the sphere intersecting with the cylinder is

$$\begin{aligned} &d_{B1} < R_A : \text{sphere intersects cylinder} \\ &d_{B1} > R_A : \text{sphere does not intersect cylinder} \\ &d_{B2} < R_A : \text{sphere intersects cylinder} \\ &d_{B2} > R_A : \text{sphere does not intersect cylinder} \end{aligned} \tag{161}$$

Configuration 2: sphere lies to "left" axial extremity of cylinder.

Figure 17 contains an illustration of the geometry for Configuration 2. Here the designation of the position of the sphere "beyond" the axial extremity of the cylinder is here in terms of the center of the sphere, $P(x_B, y_B, z_B)$, and the point on the centerline of the cylinder $P(x_{A1}, y_{A1}, z_{A1})$ as indicated in Fig. 12.

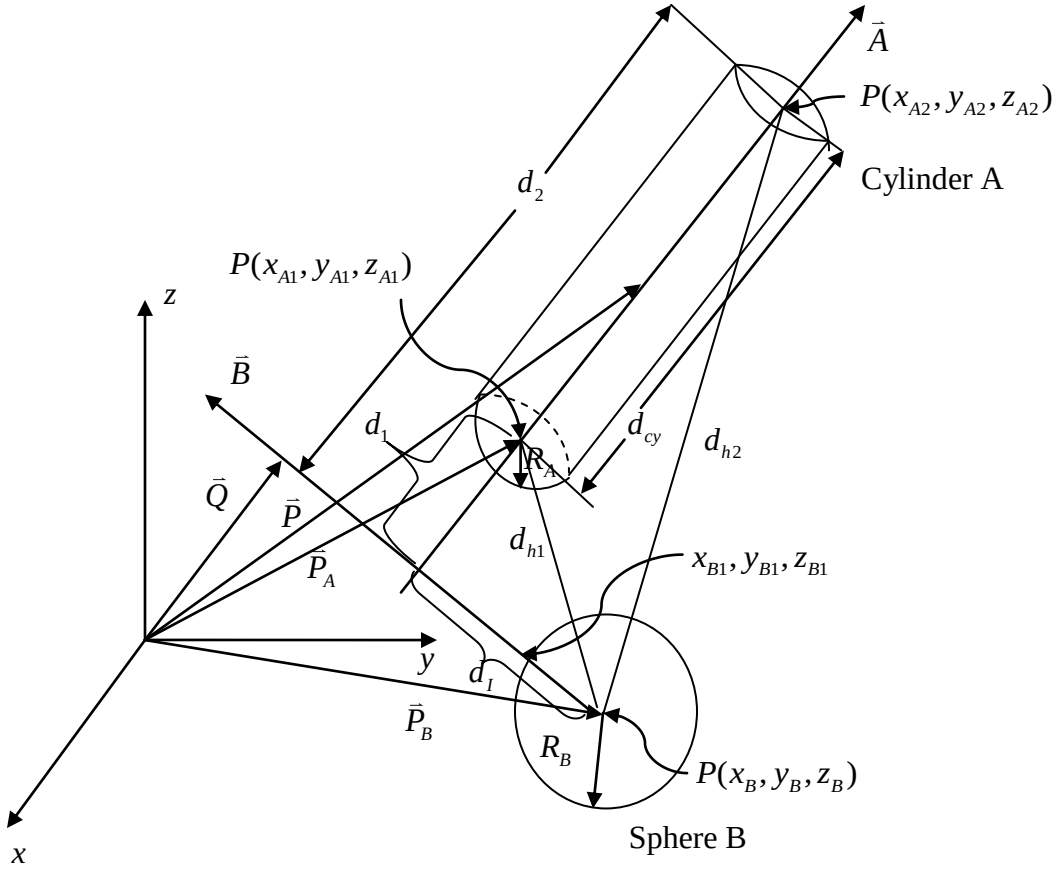

Figure 17. Collision of cylinder and sphere for Configuration 2.

For this configuration, which is illustrated in Fig. 17, the following formulations apply:

$$d_{h1}^2 = d_I^2 + d_1^2, \tag{162}$$

$$d_{h2}^2 = d_I^2 + d_2^2. \tag{163}$$

$$d_{cy} = d_2 - d_1 = \left[\left(x_{A2} - x_{A1} \right)^2 + \left(y_{A2} - y_{A1} \right)^2 + \left(z_{A2} - z_{A1} \right)^2 \right]^{1/2} \tag{164}$$

The expressions in Eqs.(162) and (163) are identical to those in Eqs.(155) and (156). The distance measure in Eq.(164) differs from Eq.(153) because the POI lies beyond the end of the cylinder. Thus, d_1 is measured between the "left" end of the cylinder and the external POI and, while d_2 is now greater than d_{cy}.

Solving Eq.(164) for d_2, substituting in Eq.(163), and solving the resulting expression and Eq.(162) simultaneously gives

$$d_1 = -\frac{d_{h1}^2 - d_{h2}^2 + d_{cy}^2}{2 d_{cy}} \tag{165}$$

and

$$d_2 = d_{cy} - d_1. \tag{166}$$

The sign in Eq.(165) is the opposite of the sign in Eq.(157), while Eq.(166) is identical to Eq.(158). The value d_1 given by Eq.(165) is used as the parameter $t = t_I = d_I$, which can be used in Eq.(148) to give the POI (x_I, y_I, z_I).

Four types of geometry arrangements are assessed to determine whether the cylinder and sphere intersect. These are illustrated in Figs. 18–21, inclusive of the distance and dimension quantities needed to determine insection.

Type 1: No intersection – no overlap.

Here $d_2 > d_{cy}$ and $d_1 > R_B$ for all d_I. The sphere is centered a distance d_1 from the end of the cylinder. The surface of the sphere at radius R_B is less than d_1; hence, no intersection occurs.

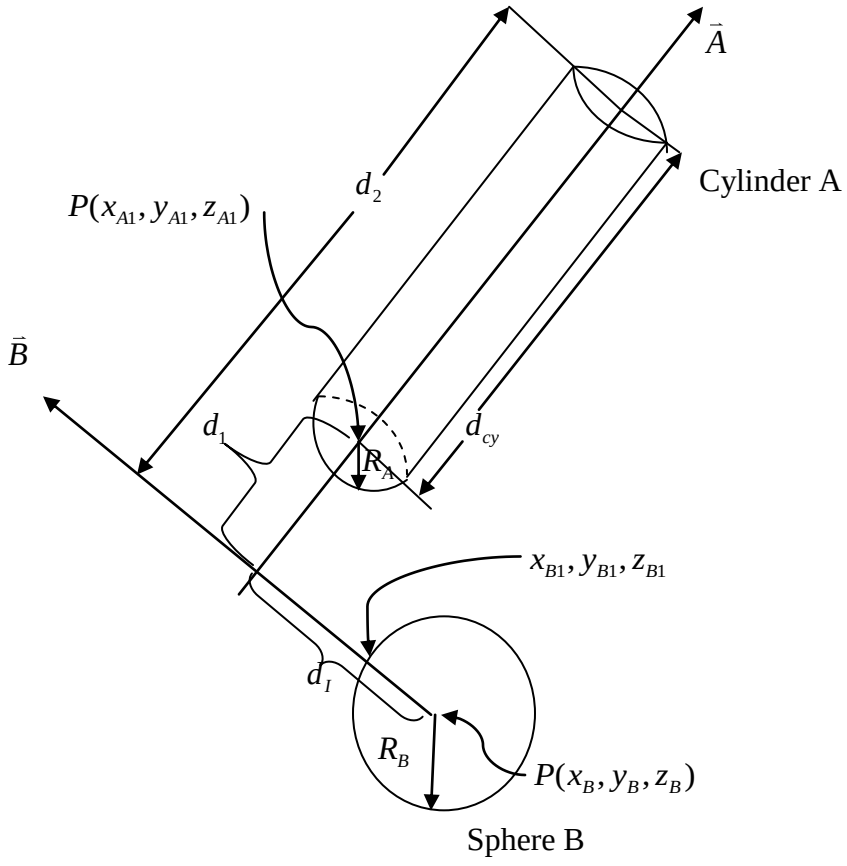

Figure 18. Collision of cylinder and sphere for Configuration 2, Type 1.

Type 2: No intersection – overlap.

Here $d_2 > d_{cy}$, $d_I > R_B$, and $d_e > R_B$. The sphere is centered a distance d_1 from the end of the cylinder. The surface of the sphere at radius R_B is greater than d_1. The distance d_e between the end edge of the cylinder and center of the sphere is greater than R_B; hence, no intersection occurs.

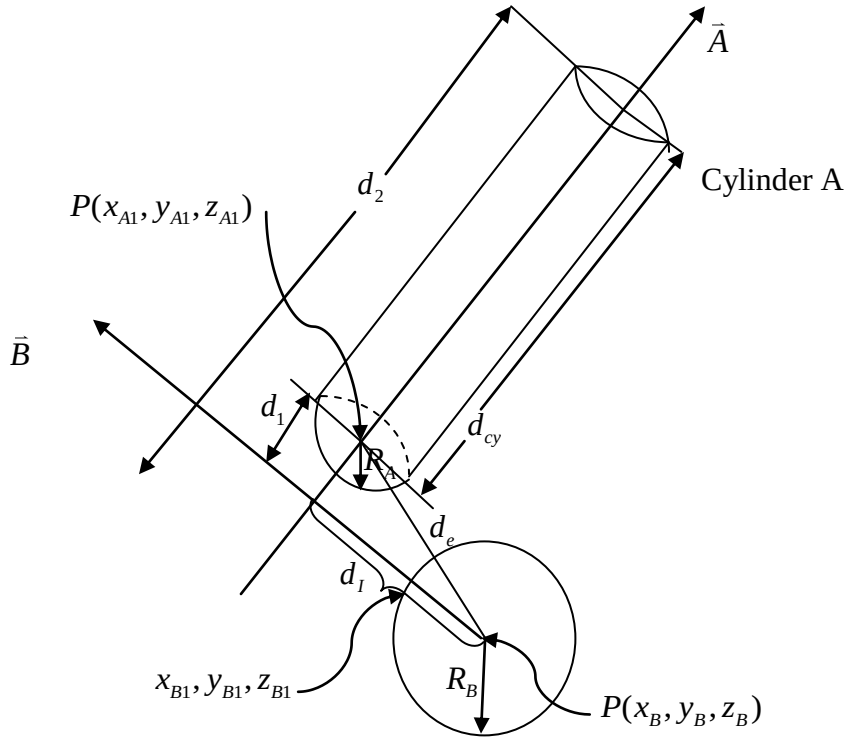

Figure 19. Collision of cylinder and sphere for Configuration 2, Type 2.

Type 3: Side-end intersection.

Here $d_2 > d_{cy}$, $d_1 < R_B$, and $d_e < R_B$, where

$$d_e = \left(d_1^2 + d_{B3}^2\right)^{1/2} \tag{167}$$

is the minimum distance between the sphere and the end of the cylinder and

$$d_{B3} = d_I - R_A . \tag{168}$$

For these conditions intersection occurs.

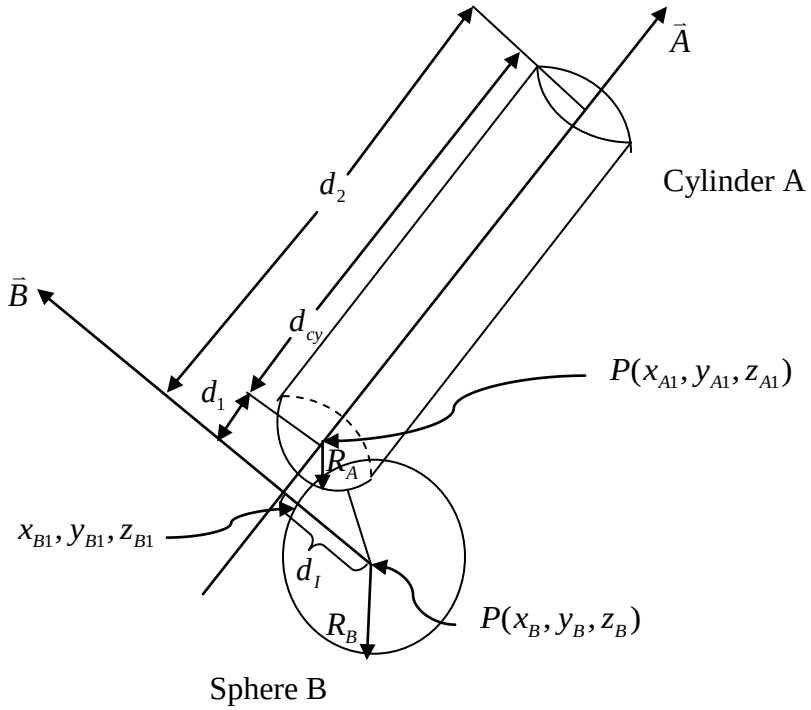

Figure 20. Collision of cylinder and sphere for Configuration 2, Type 2.

Type 4: End intersection.

Here $d_2 > d_{cy}$, $d_1 < R_B$, and $d_I < R_B$. The sphere intersects the cylinder through the surface of the plane defining the ends of the cylinder. For these conditions intersection occurs.

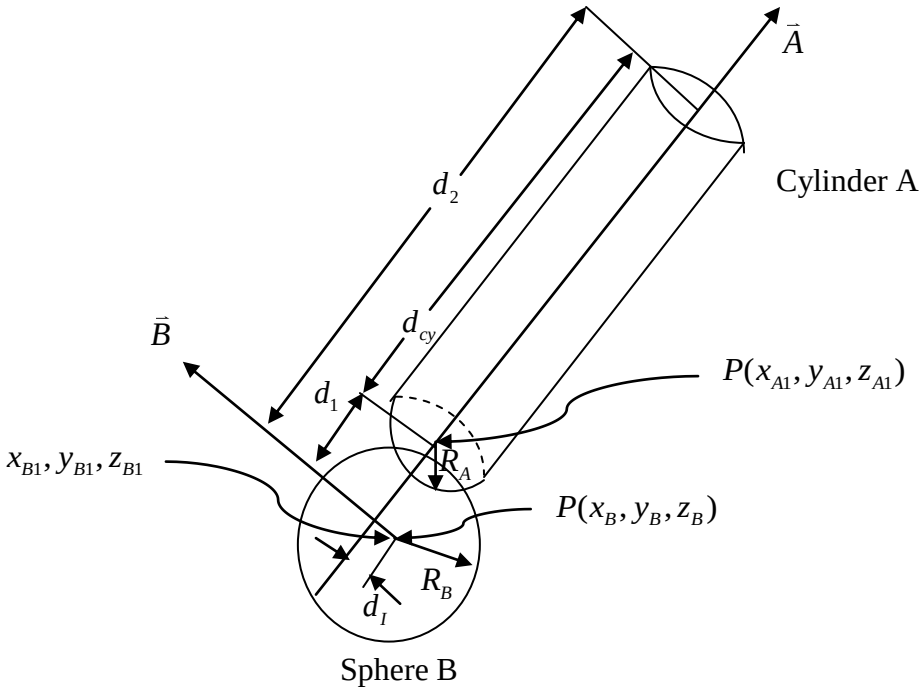

Figure 21. Collision of cylinder and sphere for Configuration 2, Type 4.

Configuration 3: sphere lies to "right" axial extremity of cylinder.

Figure 22 contains an illustration of the geometry for Configuration 3.

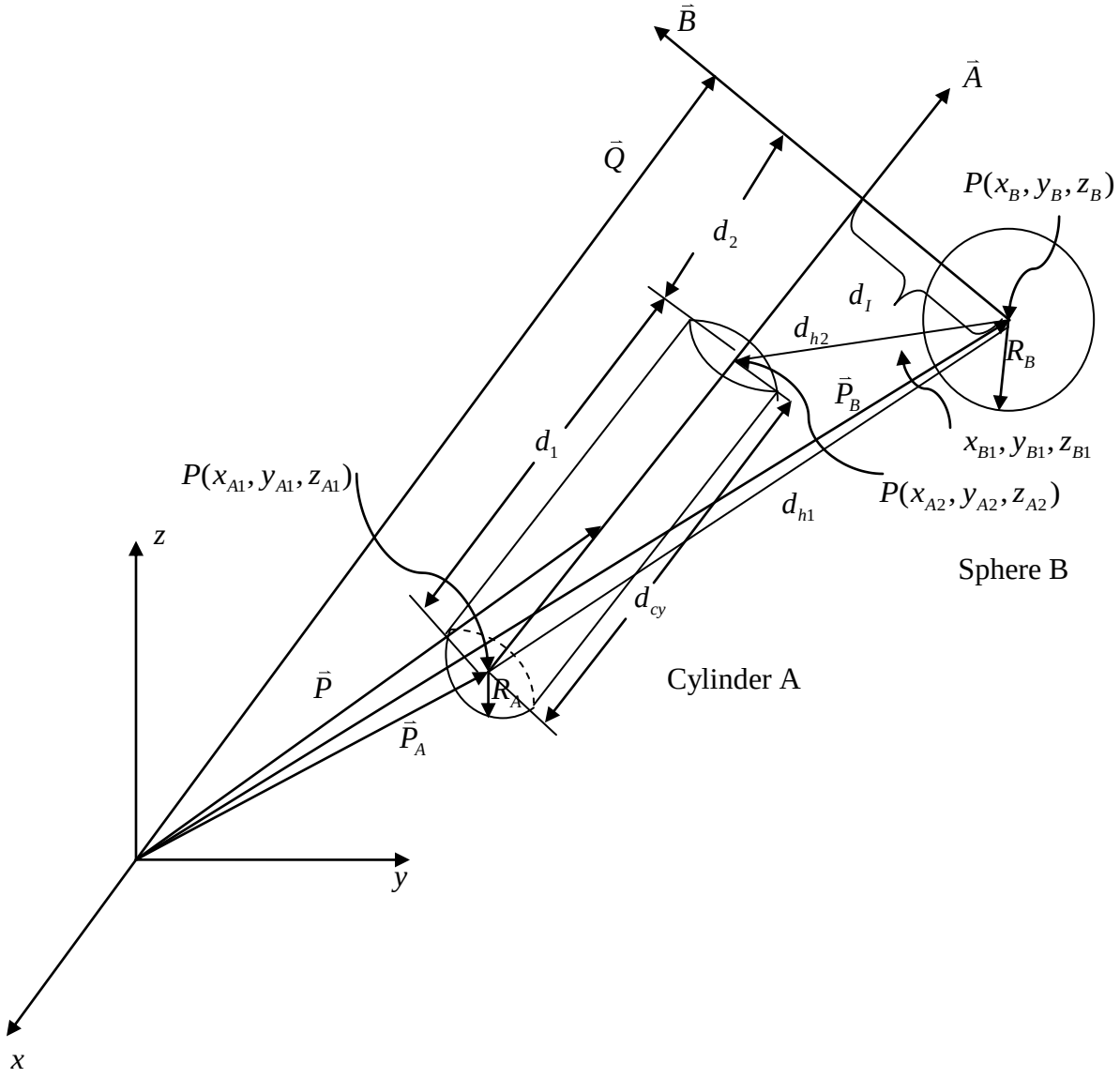

Figure 22. Collision of cylinder and sphere for Configuration 3.

For this configuration, the following formulations apply:

$$d_{h1}^2 = d_I^2 + d_1^2, \tag{169}$$

$$d_{h2}^2 = d_I^2 + d_2^2. \tag{170}$$

$$d_{cy} = d_1 - d_2 = \left[\left(x_{A2} - x_{A1} \right)^2 + \left(y_{A2} - y_{A1} \right)^2 + \left(z_{A2} - z_{A1} \right)^2 \right]^{1/2} \tag{171}$$

The expressions in Eqs.(169) and (170) are identical to those in Eqs.(155) and (156). The distance measure in Eq.(171) differs from Eq.(153) and Eq.(164) because the POI lies beyond the "right" end of the cylinder. Thus, d_2 is measured between the end of the cylinder and the external POI and, while d_1 is now greater than d_{cy}.

Solving Eq.(171) for d_2, substituting in Eq.(170), and solving the resulting expression and Eq.(169) simultaneously gives

$$d_1 = \frac{d_{h1}^2 - d_{h2}^2 + d_{cy}^2}{2 d_{cy}} \tag{172}$$

and

$$d_2 = d_1 - d_{cy}. \tag{173}$$

The sign in Eq.(172) is the opposite of the sign in Eq.(157), while Eq.(173) has the opposite sign to Eq.(158). The value d_1 given by Eq.(172) is used as the parameter $t = t_I = d_I$, which can be used in Eq.(148) to give the POI (x_I, y_I, z_I).

3.6. SPH and SPH

Proximity assessment of two spheres requires the simple calculation of the distance between the centers of the spheres in relation to their radii. The procedure is illustrated in Fig. 23.

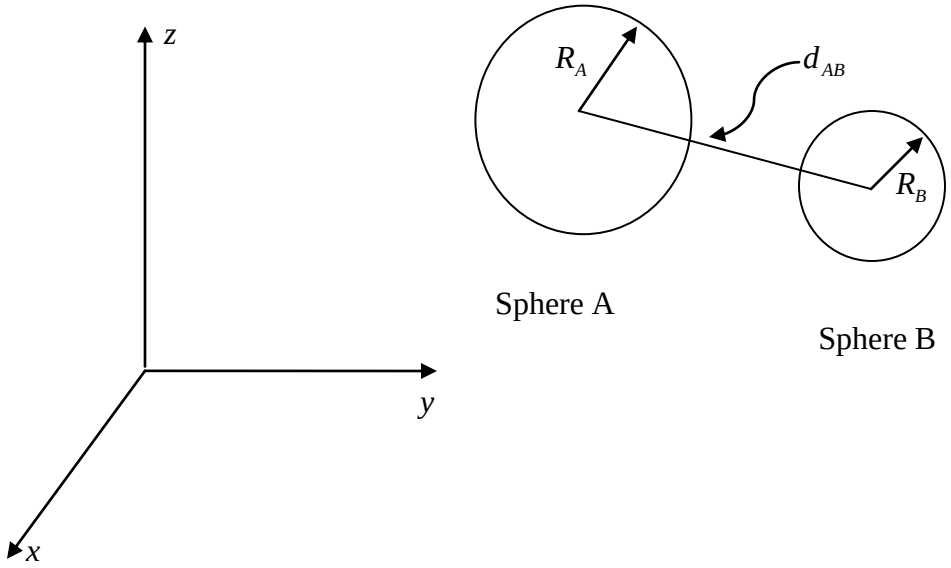

Figure 23. Determination whether POI_{A1} lies between the ends of RCCs A and B.

The PDS is

$$\begin{aligned} d_{AB} &> R_A + R_B \text{ no intersection} \\ d_{AB} &\le R_A + R_B \text{ intersection} \end{aligned} . \qquad (174)$$

4. SUMMARY AND CONCLUSIONS

The Los Alamos TRX code is being developed as front-end to the MCNP6 Monte Carlo radiation-transport code to facilitate model creation and execution using a user-friendly graphical user interface. The TRX graphics tool will plot geometry, but should also have the knowledge to understand object proximity. This knowledge is necessary for the automated creation of the geometry information required by MCNP6.

Historically, MCNP6 model preparation has required that the user determine object proximity. This process has been aided by the MCNP6 geometry plotter, which can be used to inspect geometry for flaws. This feature is not appropriate for TRX because it identifies intersections of surfaces with each other and the plot plane and draws the resulting curves. Hence, there is no information regarding object proximity other than that generated for a designated plot. MCNP6 geometry can also be assessed using particle transport to detect flaws. Proximity assessment is limited specific points, and portions of the geometry may not experience particle transport so that all of the geometry may not be assessed.

We have developed algorithms to provide suitably characterized object proximity assessment capability to TRX. We have avoided algorithms that iteratively assess proximity. Moreover, the algorithms are also designed to provide a prescription to reposition an object that is determined to collide with another object. Thus, the expressions are not developed by simple simultaneous solution of the equations for two surfaces. Instead, equations of lines between two surfaces are used to provide a characterization of the minimal distance between surfaces. Objects can then be separated using a single parameter for the equation of the line. With one exception, the

algorithms are deterministic and analytic. A numerical solution is required for the case of an intersecting ellipse and circle.

REFERENCES

Brown F.B., ed., April 2003, "MCNP–A General Monte Carlo N–Particle Transport Code, Version 5, Volume I: Overview and Theory," Los Alamos National Laboratory report LA-CP-03-0245, Ch 2 pp. 182–185.

Tierney J.A., 1974, *Calculus and Analytic Geometry*, Allyn and Bacon, Inc., Boston, p. 434.

Trench W.F. and Kolman B., 1972, *Multivariable Calculus with Linear Algebra and Series*, Academic Press, Inc., New York, pp. 412–423.

Wolfram S. (1991), *Mathematica*, Addison-Wesley, New York, Second Edition, pp. 121–124.